August 2018

Effects of Metal Sulfate Electrolyte Additives on Charge Acceptance in Agm Batteries

Alex Drake
University of Wisconsin-Milwaukee

EFFECTS OF METAL SULFATE ELECTROLYTE ADDITIVES ON CHARGE ACCEPTANCE IN AGM BATTERIES

by

Alex Drake

A Thesis Submitted in

Partial Fulfillment of the

Requirements for the Degree of

Master of Science

in Engineering

at

The University of Wisconsin-Milwaukee

August 2018

ABSTRACT

EFFECTS OF METAL SULFATE ELECTROLYTE ADDITIVES ON CHARGE ACCEPTANCE IN AGM BATTERIES

by

Alex Drake

The University of Wisconsin-Milwaukee, 2018
Under the Supervision of Professor Deyang Qu

In the United States the transportation sector is the second largest source of greenhouse gas emissions, making up 27% of the total greenhouse gas emitted in 2015. Within the transportation sector passenger vehicles make up the largest percentage of emissions at 41.6% [1]. To help curb passenger vehicle CO_2 emissions manufacturers are adopting increasing amounts of hybrid technology. Micro-hybrid technology utilizes a typical internal combustion engine and lead-acid battery partnered with Start-Stop technology and regenerative breaking to decrease emissions by 5-12%. To keep up with the electrical demands of this type of use, advanced lead acid batteries in the form of Absorbent Glass Matt (AGM) batteries are being used in these systems. With an ever-growing electrical demand placed on these batteries, improvements to the charge acceptance of these batteries is required. Much research is being done on adding carbon materials to the batteries lead plates and various compounds to the electrolyte to increase charge acceptance. For the original experiments contained in this paper, the use of metal ion sulfate salts to improve charge acceptance is investigated. Results establish that different metal ions and different concentrations of ions have a broad range of effects on charge acceptance. Magnesium, zinc, and aluminum ions showed a 32-41% increase in charge acceptance at a 60% state of charge.

TABLE OF CONTENTS

ABSTRACT ii
LIST OF FIGURES iv
LIST OF TABLES v
1 Introduction 1
1.1 Energy Storage 1
1.2 History of the Lead Acid Battery 1
1.3 Lead Acid Battery Chemistry/Mechanism 3
1.4 Differences in Current Lead Acid Battery Technology 4
1.5 Requirements for Batteries in Micro-Hybrid Applications 7
1.6 The Case for Lead acid over other technology, AGM Tech in Micro Hybrid Applications, and Needed Improvements 11
1.7 State of Research 18
1.8 Increasing Micro-Hybrid capability through Negative/Positive Paste Additions 19
1.9 Increasing Micro-Hybrid capability through Changes in Electrolyte Composition 30
2 Experimental 43
2.1 Methods and Materials 43
2.2 Electrical Tests 47
2.3 Analytical Tests 51
3 Results and Discussion 53
3.1 Charge Acceptance 53
3.2 Cold Cranking 58
3.3 ICP-OES Analysis 59
3.4 SEM and EDS Analysis 62
4 Conclusion 65
4.1 Future Work 66
Works Cited 69
Appendix: Charge Acceptance and Cold Cranking Raw Data 74

LIST OF FIGURES

Figure 1-Plante original lead acid battery [3] 2
Figure 2-ALABC battery markets 2013 [5] 2
Figure 3-Main Lead Acid battery chemical equations. 3
Figure 4: AGM Battery Exploded View 7
Figure 5:HRPSoC cycling on activated carbon samples [36] 22
Figure 6: Carbon additive effect on HRPSoC Cycling [36] 24
Figure 7: 5000x magnified SEM images of (A)commercially available CNTs. and (B)Molecular Rebar [38] 26
Figure 8: Cold charge acceptance test 27
Figure 9: EUCAR Power Assist Life Cycle Test[40] 29
Figure 10:Chelating additive Na_2EDTA mechanism with lead sulfate.[52] 36
Figure 11:PSoC cycling profile. 39
Figure 12: Conversion indicator performance under PSoC cycling. 40
Figure 13-Sodium Ion Concentration 43
Figure 14: Single cell construction. A) Empty battery box. B) Battery box with plate stack. C) Completed box front. D) Completed box back. 47
Figure 15:AGM Lead-Acid Battery Formation Plot 48
Figure 16:Failed Lead-Acid Battery Formation 49
Figure 17:5 Cycle Test 50
Figure 18: Negative Plate Sample Locations 53
Figure 19: High Concentration Dynamic Charge Acceptance plot, All Acids 53
Figure 20:Charge acceptance plot for magnesium across four different DoDs 54
Figure 21: Aluminum Sulfate Charge Acceptance for several concentrations 55
Figure 22: Zinc Sulfate Charge Acceptance for Several Concentrations 56
Figure 23: Charge acceptance of Metal-Ion Sulfates at the 0.035 M level 57
Figure 24: Charge acceptance plot for 0.0351 M magnesium across four different DoDs. 58
Figure 25: Cold cranking capacity of low concentration acids. 59
Figure 26: SEM images of negative lead plate. (A) Zinc low concentration, location 2, (B) Zinc low concentration, location 3, (C) Aluminum low concentration, location 2, and (D) Aluminum low concentration, position 3. 63
Figure 27: EDS spectra for the no additive negative plate. 64
Figure 28:Lead sulfate crystal formation.[60] 68

LIST OF TABLES

Table 1 Carbon and Lamp Black Characteristics 21
Table 2:Surfactant properties. 38
Table 3:Table of Sulfate Salt and Acid Properties. The table shows the properties for acids containing (A) Sodium Sulfate, (B) Magnesium Sulfate, (C) Aluminum Sulfate, (D) Lithium Sulfate, (E) Zinc Sulfate, (F) Indium Sulfate, (G) Copper Sulfate, (H) Bismuth Sulfate, (I) Tin Sulfate, and (J) Potassium Sulfate. 44
Table 4: Properties of Zinc Sulfate-Sulfuric Acid Solutions 44
Table 5: Properties of Aluminum Sulfate-Sulfuric Acid Solutions 45
Table 6:Acid properties at low levels of metal ion additives. (A) Magnesium Sulfate, (B) Aluminum Sulfate, (C) Lithium Sulfate, (D) Zinc Sulfate, (E) Indium Sulfate, (F) Copper Sulfate, (G) Bismuth Sulfate, (H) Tin Sulfate, and (I) Potassium Sulfate. 45
Table 7: ICP-OES results for aluminum content of electrolyte at 300 times dilution. 60
Table 8:ICP-OES results for zinc content of electrolyte at 300 times dilution. 60
Table 9: ICP-OES results for zinc, aluminum, and lead concentration in lead plates 61
Table 10: Raw Data for 0.2112 M Charge Acceptance Plot 74
Table 11: Raw Data for Aluminum Acids Charge Acceptance Plot 74
Table 12: Raw Values for Zinc Charge Acceptance Plot 74
Table 13: Raw Values for 0.0352 Charge Acceptance Plot 75
Table 14: Cold Cranking Raw Values 75

1 Introduction

1.1 Energy Storage

For as long as man has been generating electricity there has been the desire to store it. The man credited with creating the first battery in 1800 used zinc and copper discs, a cardboard separator, and a brine electrolyte [2]. Fast forward 200 years and batteries have found their way into nearly all aspects of life. From starting cars to powering cell phones and running smoke detectors, batteries have become an integral part of the modern world. This widely versatile technology's influence will continue to grow as the demand for electricity continues to grow. One subset of the battery industry, the AGM battery, has an interesting role to play in society's energy future.

1.2 History of the Lead Acid Battery

The original battery created by Alessandro Volta was what is known as a primary cell. In a primary cell, once the positive and negative active materials no longer have a high enough voltage difference, the battery can no longer be used. The next logical step in battery development was a battery that could be reused many times (secondary cell). In 1860 the French scientist Gaston Plante solved this problem when he created the first lead acid battery [3].

The lead-acid battery designed by Plante, which consisted of nine cells in series, as seen in Figure 1 was the only secondary cell until the creation of the nickel-cadmium battery 40 years later. Unlike the nickel-battery, lead acid batteries have managed to remain one of the dominant energy storage technologies for well over 100 years.

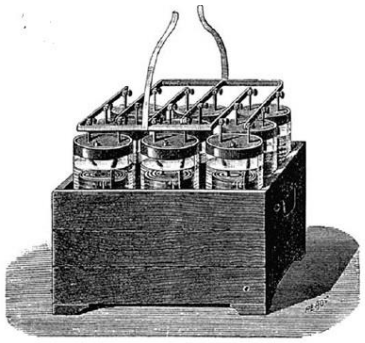

Figure 1-Plante original lead acid battery [3]

There are many factors that have led to the prominence of lead-acid technology over other secondary battery types. The two main factors behind lead acids success is the low cost of lead and it's versatility [4]. The cost of lead has always been low, and in comparison to the high cost of components in competing battery technologies like lithium-ion, it often provides enough of an and edge to maintain its place. The versatility of the lead acid battery can be clearly seen today by its wide use in a variety of applications. While most people may only be familiar with lead acid batteries because of their use in automobiles, they can also be found in many other places. Figure 2 highlights that lead acid batteries play a prominent role in not only the automotive market, but also in telecommunications and backup supply markets.

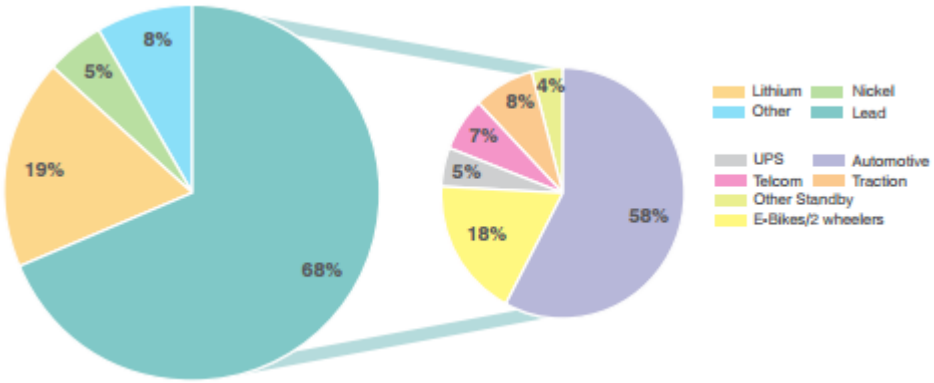

Figure 2-ALABC battery markets 2013 [5]

1.3 Lead Acid Battery Chemistry/Mechanism

Since the lead acid battery's inception over 150 years ago, little has changed with the basic setup of the battery, with the main components still having the same requirements. There are four main components of any successful battery: a cathode and anode, a separator, an electrolyte, and a load. As with any redox (reduction-oxidation) reaction, an oxidation reaction occurs at the anode, resulting in free electrons that then flow through the load to the cathode where the electrons are consumed in a reduction reaction. Below the reaction equations show the process by which the chemical reaction in the lead acid battery occurs.

Anode Reaction (-): -0.356 V

$$Pb_{(s)} + HSO_{4\,(aq)} \rightarrow PbSO_{4\,(s)} + H^{+}_{(aq)} + 2e^{-} \qquad \text{Eq. 1}$$

Cathode Reaction (+): 1.685 V

$$PbO_{2\,(s)} + HSO_{4\,(aq)} + 3H^{+}_{(aq)} + 2e^{-} \rightarrow PbSO_{4\,(s)} + 2H2O_{(l)} \qquad \text{Eq. 2}$$

Total Reaction: 2.041 V

$$Pb_{(s)} + PbO_{2\,(s)} + 2H_2SO_{4\,(aq)} \rightarrow 2PbSO_{4\,(s)} + 2H_2O_{(l)} \qquad \text{Eq. 3}$$

Figure 3-Main Lead Acid battery chemical equations.

The reactions above show the discharge reaction for a lead acid battery. As a secondary battery, the reverse reaction takes place during recharge when outside energy is applied to the system. For use in today's automobiles a single cell, which provides about 2.2 volts, is not enough. A stack of 6 cells is required to meet the requirements of 12 V systems used in most automobiles.

The second main component in the lead acid battery is the electrolyte. For lead acid batteries, the electrolyte is a sulfuric acid solution. The reactions listed above show that the

sulfuric acid provides the necessary compounds, in the case HSO_4, to allow the oxidation and reduction reactions to happen simultaneously. An interesting note about reactions taking place inside the lead acid battery is what happens when the battery is fully discharged. Since both plates result in the formation of $PbSO_4$ (lead sulfate) during discharge, the acidity of the electrolyte decreases during discharge, with almost no acid remaining in a fully discharged cell. Because of this fact, testing the density of the electrolyte is often used to check the health flooded cells.

The third main component of a lead acid battery is the separator. The main role of the separator is to prevent an electrical short circuit from forming between the positive and negative plates, but it must also be resistant to sulfuric acid and allow for ionic transport through the separator. The earliest separators, like those used by Plante and his peers, were often made of substances such as natural rubber and cardboard [2]. As time went on, changes were made to the separator materials from things like rubber, sponges, cork, and wood. From around 1880 through the 1940's wood was used until cellulose and PVC separators became the norm [6]. The next big change in lead acid battery design came in the 1970's with the invention of the AGM battery [7].

1.4 Differences in Current Lead Acid Battery Technology

Today, there are four main types of lead acid batteries available and are most easily distinguished by their separator style. The flooded style is the oldest and most common. These batteries utilize a solid separator, typically a material like polyethylene [6]. The acid electrolyte fills the body of the battery case keeping the lead plates completely submerged in acid. These batteries represent the least expensive type and have been used in automobiles for decades. The main drawback with this style of battery is that there is no system in place for oxygen and

hydrogen recombination. This results in the gradual loss water from the battery and, without proper maintenance, a shorter life span.

The second type of lead acid battery today is an Enhanced Flooded Battery (EFB). Similar in its overall design to the standard flooded battery, the EFB also uses a hard separator and fills the battery case with acid, keeping the plates constantly submerged. The main difference between standard flooded batteries and enhanced flooded batteries lies in the lead plates themselves. EFBs use carbon additives to improve charge acceptance and cycle life [8].

The third variant of lead acid batteries is the gel lead acid battery. Very different from the flooded batteries mentioned above, the gel lead acid battery uses the addition of silica to the electrolyte to create a gel [6]. This type of battery is one that falls into the category of Valve Regulated Lead Acid Batteries (VRLA). In VRLA batteries, the battery case is sealed with a pressure release valve to prevent gases from escaping at low pressures. This is done to allow for the recombination of hydrogen and oxygen inside the battery, removing the need to add water to the battery. Also known as maintenance free batteries, this feature allows for a heightened versatility. In the gel VRLAs, the gelled electrolyte will initially shrink and crack during charging causing small amounts of water loss. After these cracks have formed, they offer the pathways for oxygen generated on the positive plate to travel through the gel to the negative plate to be reduced [6].

The final type of lead acid battery to be discussed here is the Absorbent Glass Mat (AGM) VRLA. In an AGM battery a fiberglass mat is used as the separator material. These mats have a long list of positive attributes including high acid resistance, high wettability (low contact angle) with sulfuric acid, inexpensive, easily variable diameter and length of glass fibers,

and stability through a wide temperature range [9]. By changing the diameter and length of the glass fibers and the percentages of certain sized fibers, properties like pore size, surface area, and separator density can all be manipulated. These considerations are important for determining acid filling speeds and diffusion rates through the separator.

Another factor that can greatly change the behavior of an AGM battery is the level of compression experienced by the separator. The general trend with regards to separator compression is that low compression leads to shorter cycle life and that a minimum pressure of around 40kPa should be experienced at the plate/separator interface [9]. It has been noted that another important characteristic of the separator is that it is able to rebound after cycles of increasing and decreasing pressures caused by the changing plate thicknesses during charge and discharge cycles. Additionally, increasing the amount of compression of the separator will reduce the amount of acid that the mat can absorb, while adding acid to compressed mat will reduce the amount of compression due to the reduction of friction/force within the mat [9]. These characteristics of compression are important for consideration during the design of a AGM battery.

Since the lead-acid battery's creation in the mid 1800's, many changes have been made to improve the technology's usefulness., Figure 4 (below) [10] shows an exploded view of a modern AGM battery.

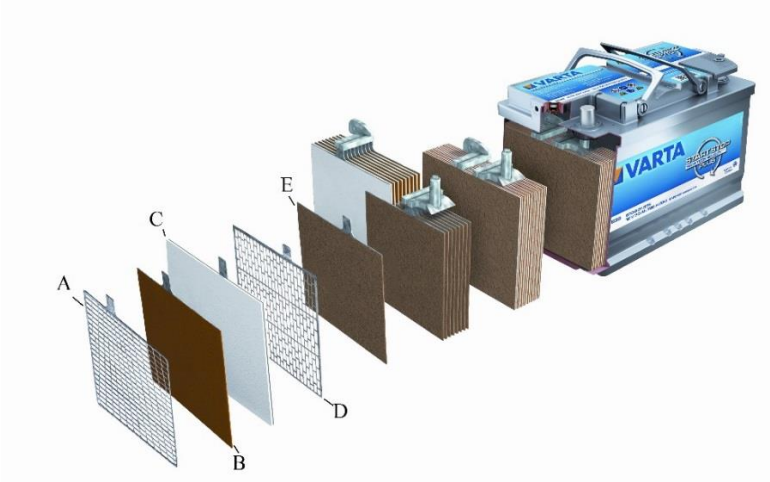

Figure 4: AGM Battery Exploded View

When comparing Figure 4 to Figure 1, the differences are clear. Instead of using coiled lead sheets separated by rubber strips [3], most lead acid batteries found in cars today use lead plates separated by various separators. In the more modern batteries, both the separators and the plates have more complicated constructions and purposes. The positive and negative plates, labeled as B and C respectively in Figure 4, are combinations of lead and other materials pressed around a metal grid. This grids, A and D (Figure 4), act as the current collector and are responsible for conducting the electricity from the terminal to the plate's active material, allowing for electricity to be stored in chemical bonds. The final part focused on in Figure 4, is the separator (part C). The diagram shows the use of an AGM separator and will be the separator of choice for the testing to follow.

1.5 Requirements for Batteries in Micro-Hybrid Applications

In the United States and around the world, serious consideration is being giving to the issue of CO_2 emissions. Across numerous industries methods are being employed to reduce the amount of CO_2 and other greenhouse gases emitted. These methods range from CCS (carbon capture and sequestration), to wind and solar generation, to driving more efficient or electrified

automobiles. All of these methods would reduce CO_2 emissions, but questions of cost and efficiency must also be considered.

Many car manufactures like Tesla, with its completely electric line of vehicles, and Nissan, with its all electric Leaf, have begun focusing on reducing the need for oil by removing internal combustion engines altogether. While on the surface this appears to be a win for the environment, an immediate shift from gasoline to electric cars would merely shift the CO_2 emissions from the tailpipe to the power plant, where in the United States almost 65% of electricity generated is done so using fossil fuels like coal and natural gas [11]. The use of electric cars is an important step toward improving the way people are transported, but until the electricity used to power these cars is generated using renewable methods, it will not be the solution.

Another way to reduce automotive carbon emissions and to meet the ever-tightening government pollution restrictions is to increase the overall efficiency of today's automobiles. Several methods being introduced to boost internal combustion engine (ICE) efficiency without redesigning the engine include reducing idle rpm, mild to full drivetrain hybridization, and the utilization of micro-hybrid technology [12]. Full hybridization of the drivetrain does result in the greatest reduction in CO_2 emissions, but also has the highest cost per pound of CO_2 reduced [12]. The cost/reduction ratio is lowest at lower levels of hybridization and higher at higher levels of hybridization. Keeping in mind that automotive companies are businesses, the most likely goal of reducing emissions will be doing so for the lowest cost.

This is where micro-hybrid technology comes into play. There are four main components that make up micro-hybrid technology; Start/stop functionality, regenerative breaking, charge voltage control, and passive boost [13]. These four systems can be used individually or in

concert with one another, with changing battery requirements based on which systems are used. The theory behind start/stop functionality is simple; cars cannot burn fuel while idling if the engine is not running. When the car is stopped or hits a certain low speed, the engine will be automatically shut off to conserve fuel. While stopped, all the electrical features that are typically powered by the alternator during vehicle operation are instead powered by the battery. When the gas pedal is depressed, the engine is quickly restarted and standard operating behaviors continue. The added stress that this function adds to the battery is the added drain of supplying electricity to the electronic features while the engine is not running and being able to start the engine many times instead of once per trip. With just the start/stop segment of micro-hybrid technology in play, fuel savings land around 6% [13] and in the range of 5-10% [10] when compared to the same model care without start/stop technology.

The second component of micro-hybrid technology is regenerative braking. The goal of a regenerative braking system is to capture the kinetic energy usually lost during the breaking process and turn it into potential energy. In the case of automobiles, the kinetic energy is transformed into electricity and used to charge the battery. In standard cars, the method used to stop a car is hydraulic breaking. When the brake pedal is depressed in the car, fluid is forced through the brake lines causing the brake pads to close on the brake rotor. The result is a lot of heat and a slowed or stopped car. For a regenerative system the alternator, or a separate electric motor, is designed to run by the rotation of the wheels during breaking, using the cars momentum to generate electricity instead of energy from the engine. Using these systems some of the energy that would typically be lost as heat can instead be stored as electricity in the battery. Much like the start/stop feature mentioned above, regenerative breaking creates additional requirements for the battery.

One of these new requirements is for a lower target operating State of Charge (SoC) [13] Standard Starting, lighting, Ignition (SLI) batteries typically remain around 100% state of charge. When operating at a high state of charge, the ability for a battery to accept charging energy, commonly known as charge acceptance, is very low. To utilize the energy from regenerative breaking, the battery needs to operate at a lower SoC to be able to maximize the energy recovered from regenerative breaking. The second new requirement is that the battery needs to have a higher overall dynamic charge acceptance over current SLI batteries.

The last two features of micro-hybrid technology are charge voltage control and passive boost. Charge voltage control is a system that works to keep the energy needed to recharge the battery as low as possible while also ensuring that the battery is never overcharged [13]. This is achieved by reducing the charging voltage and not charging the battery while idling. The passive boost feature acts to stop the alternator from producing electricity during acceleration. This reduces the fuel consumption needed to increase the cars speed by removing the energy drain from the alternator. The effect this has on the battery is an increase in charge and discharge cycling since the battery must run the electrical features during acceleration instead of the alternator [13].

1.6 The Case for Lead acid over other technology, AGM Tech in Micro Hybrid Applications, and Needed Improvements

1.6.1 Lead Acid vs Lithium Ion

The dominant battery technology for automobiles has always been the lead acid battery. But with the prevalence of lithium ion batteries (LIBs) in people's daily lives, many may wonder why would investments be placed in an old technology like lead acid batteries for cars when something better is already here. While it is true that lithium ion batteries do have many attractive qualities like high cycle life, energy efficiency, and high energy densities, the temperature issues, recyclability, cost, and availability of materials cause issues when looking to expand their uses in automotive markets. The largest issue is, however, not a technical one but a marketing one. People need to buy electric cars for the market to be successful.

One major issue to consider when looking at lithium ion and lead acid batteries for cars is the temperature range in which they will be operating. For most lithium ion technologies there is a dramatic decline in their performance around the 0˚ C (32˚ F) and another dramatic drop at temperatures below -20˚C (-4˚F). At these very low temperatures the chemical reaction is slowed almost to a stop [14]. Simply put, lithium ion batteries struggle to perform at colder temperatures like those experienced in the winter months in the northern United States. Lead acid batteries, however, can operate in these cold temperatures and meet the needs of a modern automobile.

Another concern that growing lithium ion use raises is recyclability. The compounds that are found in typical lithium ion cells changes depending on what chemistry the electrodes use, but can contain cobalt, lithium, nickel, manganese, and iron. The recycling rates of the materials found in LIBs is different for each element. The focus on LIB recycling has mainly been to

retrieve the cobalt and nickel from spent batteries. Recycling efficiency for these metals is around 50% while the lithium recycling efficiency is less than 1% [15][16]. The main issues that increase the difficulty of recycling LIBs include the large list of compounds in the battery, high cell count in the batteries, and the different construction materials and methods between different manufactures. Lead acid batteries on the other hand, have a very successful recycling network already in place. Currently, lead acid batteries are recycled at a higher rate than any other consumer product in the United States with a recycling rate around 99% [8].

A close issue with recycling is material availability and cost. Should a major switch to lithium ion batteries take place for powering automobiles the availability of necessary components to fulfill the demands of such a large market, in addition to meeting the needs of an ever-growing portable electronics market, could become an issue. One example of this trend appeared between 2005 and 2010 when the U.S. lithium consumption for batteries increased 194% [17]. Another can be seen more recently with the increase in costs of lithium imported to China where in the May of 2016 the costs had risen 42% in the preceding 6 months [18]. The cost and availability of lithium alone is not the only issue that may impact lithium ion's future in the automotive industry.

Another main component found in many lithium ion batteries is cobalt. Cobalt is used as a main component in the cathode material in several different lithium ion chemistries including lithium cobalt oxide (LCO), nickel cobalt aluminum (NCA), and nickel manganese cobalt (NMC) [19]. Each chemistry gives different performance in terms of energy density, power density, and capacity so certain chemistries are better suited to different applications. Most portable electronics use LCO batteries and Tesla, one of the most visible names in the electric vehicle market today, uses NCA batteries to power its vehicles [20]. The portable electronics

and automobile markets are both likely to experience huge growth in the coming years and companies are already planning to secure cobalt supplies for their batteries.

Bloomberg, among other news outlets, has reported that Apple is one company among many seeking to set up direct supply lines with mining companies to ensure cobalt is available for their battery production [21]. The main reason given for this move is fear of availability because of the expected growth in the electric vehicle market. Other companies including Samsung SDI and Volkswagen AG are also making deals to ensure their cobalt supply over the next several years. An additional issue surrounding the production of cobalt lies with the political stability and unethical mining practices of the Democratic Republic of the Congo, where around over half of the global cobalt supply currently originates [19] [21].

Beyond the ethics of cobalt mining, the cost of this material alone has been rapidly increasing. With the heavy increase in demand from lithium battery manufacturing, the cost of cobalt has tripled between September of 2016 and February of 2018 [21]. Concerns about further cost increases and availability exist with an increase in electric vehicles since the battery for a car requires potentially 1,000 times the cobalt of a hand held device [22]. With the high costs and possible political issues surrounding it, cobalt remains a large factor in future costs of many lithium ion batteries. In contrast to these lithium batteries, lead-acid batteries do not see these same issues with high cost fluctuations and increases with its component parts.

The last technical issue facing the large-scale implementation of the electric vehicle with lithium ion batteries is the lack of infrastructure to support electric vehicles. Tesla has built a network of charging stations across the US in major cities and along major highways to support its growing fleet of cars nationwide. The issues this system can still experience are long charge

times (30 min with supercharge) [23], restriction to areas with charging stations, and added difficulty of long distance travel. Improving fuel efficiency through, among other things, micro-hybrid technology would best utilize the existing infrastructure while allowing for new electric based infrastructure to grow and eventually meet the demands of fully electric vehicles.

The final hurdle for a successful full electric car market is getting consumers to buy into it. While resolving issues with the sustainability of EV battery recycling, convenient charging locations, and manageable purchase price will increase interest in electric cars, there are a few main issues still preventing its success; perceived safety and changing people's habits. Every few years an incident comes along that makes Li-ion batteries seem dangerous. Tesla has been at the center of the Li-ion safety controversy as early as 2013 and as recently as June 2018 for battery backs that have caught fire from road debris damage, high-speed accidents, and technical issues [24]–[27]. Samsung also experienced repeated issues with Li-ion batteries in their Galaxy-Note 7 that was eventually banned by the FAA for use in airplanes [28]. Li-ion battery fires also grounded the entire US Boeing 787 fleet until the specific causes of the battery fires could be found [29]. These incidents, while not occurring at rates higher than ICE cars, gain extra media attention and have an influence on people's perception of the technology.

Looking at the current trends in EV sales is a telling method at determining public opinion. In 2016, the percentage of completely electric vehicles sold in the us was only 2.9% [1]. The sales of cars with micro-hybrid technology, however, have shown a much more impressive growth over the past few years. Micro-hybrid systems are already found in 38% of vehicles produced between US, European, and Chinese markets and that value is expected to reach 57% by 2020 [8]. The two likely factors behind this trend are the costs associated with each technology and how it changes the way people use their cars.

First looking at price, many electric cars are already prohibitively priced for most consumers with low end EVs like the Nissan Leaf costing just under 30,000 dollars [30] and a Tesla, the brand most often referenced when discussing EVs, has cars ranging from 35,000-70,000 dollars and up depending on the model [23]. Many manufactures like Ford and GM are actively employing micro hybrid technology in many of the cars across the full range of prices with little added cost.

Based on how people use their vehicles, it is easy to see why few people are investing in electric vehicles. With an electric vehicle, special attention must be given to charge levels and the distance needed to travel and the availability of charging stations along your route. With micro-hybrid vehicles, nothing changes from the user's perspective.

Lithium ion batteries are currently used in a wide variety of technologies including a growing electric vehicle market, but are not yet ready to remove the lead acid battery from the automotive market. These Li-ion batteries have a range of issues both technical and political/environmental that need to be addressed. Low temperature performance, poor recyclability, safety, and the costs and availability of components are all issues facing the use of Lithium ion batteries in electric vehicles. These issues highlight the fact that lithium ion batteries have yet to replace the usefulness of lead acid batteries for automobiles, and that focusing on micro-hybrid cars while EV's become a more viable choice for a larger portion of the market is the best way forward.

1.6.2 AGM for Micro-hybrid

As mentioned earlier, one successful method of reducing carbon emissions is micro-hybrid technology. Micro-hybrid technology focuses on better management of the energy your car generates. Here, the focus will be on start-stop functionality and regenerative braking. Stop-

start technology shuts off the motor while the vehicle is stopped, removing the use of gasoline during typical idle conditions like sitting at a stop light or stuck in exceptionally slow-moving traffic. The regenerative braking typically uses an electric motor to generate high current loads during breaking to charge the battery. The use of these two features, in addition to battery power running the electronics while the vehicle is not moving, add some very specific requirements to which AGM batteries are better suited than standard flooded batteries. These requirements are the ability to operate at a partial state of charge (PSoC) and having a high dynamic charge acceptance (DCA) capability.

The current battery used in a typical internal combustion engine powered vehicle is an SLI flooded lead acid battery. These batteries are designed to provide the energy needed to start the car and power electronics while the vehicle is not running. This type of battery is intended to be used for a short period of time to a low depth of discharge (DoD) before being recharged and kept at a full charge. One of the most prominent issues with running a flooded cell at a PSoC is acid stratification. When a lead acid cell is fully charged the electrolyte is comprised primarily of an acid with a uniform density. As the battery is discharged and the sulfate precipitates on the plate surface, the electrolyte's water composition increases causing a change in density. This density shift will cause the denser acid to sink to the bottom of the battery forming a concentration gradient in the cell. This process occurs regularly during charging as high density sulfuric acid generated from dissolving sulfate crystals will immediately sink to the bottom of the battery.

In addition to occurring during the standard charging process, the stratification also occurs quickly if the battery is left in a PSoC, as would be common in a micro-hybrid application. The problem that stratification causes, especially during periods of rest, is the

formation of large sulfate crystals in the dense acid regions at the bottom of the plate [13]. This occurs because the plates experience a high potential in the high-density regions and low potential in the low-density regions. The result is a self-discharge reaction at the bottom of the plate causing excess lead sulfate buildup and a self-charging reaction at the top of the plate removing sulfate ions from the negative plate [13]. Once large lead sulfate crystals form, they are often too stable to be dissolved under the typical charging voltages found in an automobile and end up reducing the capacity and life of the battery. The best solution to this problem is to avoid acid stratification.

The two current options that best limit acid stratification are gelled electrolytes and the use of AGM separators. As mentioned earlier, gelled electrolytes function by adding a silica gelling agent to the electrolyte to immobilize it, which prevents acid stratification. The downside of this gelled electrolyte is poor cold weather performance. With a drop in temperature the resistance within the electrolyte increases dramatically and limits the range of applications in which gelled lead acid batteries can operate successfully [8].

Prevention of acid stratification is one main benefit of the fiberglass mats used in AGM batteries. Since the acid is held in the mat like a sponge and, it does not freely respond to gravity and cause the concentration gradients seen in flooded cells and does not have the internal resistant issues at cold temperatures seen with gelled electrolytes. As a result, AGM batteries can function for much longer periods of time at a PSoC that is necessary for micro-hybrid functionality. This, in combination with the much more efficient water recombination than that found in flooded cells, make the AGM battery perfectly suited to be the focus of continued research for lead acid batteries in micro-hybrid applications.

1.7 State of Research

As shown above, AGM batteries have come out as the dominant lead acid battery technology type for use in micro-hybrid style automobiles. That fact, when combined with growing electrical demands placed on a battery with the added features found in new cars, illustrates the need to continue improving the performance characteristics of AGM batteries. The need for continuing improvement in this technology is well known to lead acid battery industry. The Advanced Lead Acid Battery Consortium (ALABC) is a research organization with corporate members from all parts of the lead industry. The goal of this group is to improve the effectiveness of lead acid batteries in many energy storage fields.

This group has a projected goal for research during the 2016-2018 window that shows the direction of their current research. The first objective, and arguably the most important, is to increase the dynamic charge acceptance. DCA is the ability of a battery to absorb an electrical charge [31]. Currently, the lead acid battery lags behind other battery technologies in this regard and a low DCA will limit LABs role in the growing hybrid battery market.

Two more ALABC objectives are to reduce gas generation and water loss and increase the effective temperature range of LABs. The main goal of reducing gassing is to increase the life of a battery, but reducing gassing would also allow the use of greater levels of carbon additives in the plate, which have been shown to increase DCA [5]. Currently, LABs have a wider functional temperature range than Li-ion and nickel metal hydride (NiMH) batteries have difficulty with low temperature operation (less than 0˚C) but their cold weather performance is

always improving. By improving the LAB cold weather functionality, lead-acid batteries can help prevent being displaced by competing technologies.

The final two ALABC objectives for 2016-2018 deal with improving charge efficiency and reducing corrosion that is often experienced under partial state of charge (PSoC) cycling. Using higher voltages and other charging techniques would allow for faster charging of LABs, but also cause increased gassing levels that reduce battery life and DCA. This issue is closely tied with the previous objective of lowering gas generation. The final objective, minimizing corrosion under PSoC cycling conditions, is important for increasing the life of the battery. Through new additives and alloys, reduced corrosion in these conditions would result in broader versatility and lighter batteries by using thinner grids for both automotive and energy storage situations [5].

Keeping these research goals in mind, the following sections will focus on two methods for increasing the capabilities of LABs for micro-hybrid applications. The first method of interest will be the use of additives in the negative and positive plate mix. The second method, which is the method employed in the experimental portion of this paper, is through the addition of various compounds to the electrolyte. In addition to increasing the DCA of the battery, another added benefit of these methods is the minimal impact on the current design and manufacturing processes of the battery. The goal is to improve the DCA without redesigning the electrodes as seen with ultra-batteries.

1.8 Increasing Micro-Hybrid capability through Negative/Positive Paste Additions

Carbon additives are currently a very active field of research for lead acid batteries. One large motivator behind the current research is the ability of these carbon additives to slow the

formation of insoluble lead sulfate which leads to battery failure [32]. There are many different forms these carbon additives can take, and the ones looked at here are carbon black, activated carbon, carbon nanotubes, and graphitic carbon. Since each of these forms carries with it different qualities in terms of particle size, pore size, and conductivity, it is difficult to point out one specific reason or mechanism for the benefits carbon has in lead acid batteries. There are numerous possible causes for the effects of carbon including increased conductivity, prevention of large crystal growth, and the introduction of hydrogen over-potential impurities [33].

Another proposed mechanism is the formation of two separate systems on the negative plate surface; a capacitive system based on the carbon additive and the charging and discharging of a double layer and the standard chemical reaction oxidizing lead to lead sulfate [34]. Regardless of the specific mechanism, different carbon allotropes provide different results when added to a lead acid battery's negative active mass (NAM). Several of these additives and their effect on the lead acid battery's performance are discussed below.

1.8.1 Carbon Black and Activated Carbon

When using the standard plate mix absent of any additives, standard SLI and deep cycle batteries often accumulate lead sulfate crystals that do not dissolve under normal charging conditions. The results of this lead sulfate crystal growth are lower capacity, charge acceptance, and a shorter lifespan. There are many carbon based additives that have found their way into the NAM to improve battery properties and the first to be discusses are activated carbon and carbon black.

When adding either of these carbon materials to the plate mix there are several things to consider. These considerations include particle size, porosity, resistivity, degree of order, and the impurities present in the carbon [35]. Table 1 below shows four carbon black compounds and a lamp black compound and their respective values for many of the above parameters.

	CB 1	CB 2	CB 3	CB 4	LB
BET-SURFACE ($\frac{m^2}{g}$)	243	58	54	153	29
NAM MASS PERCENTAGE	0.2	1.0	1.1	0.3	2.0
AVE. PARTICLE SIZE (μm)	3.8	4.2	6.2	0.05	2.1
PORE VOLUME ($\frac{cm^3}{g}$)	0.51	0.20	0.19	0.71	0.05
ORDER (L_a, nm)	1.5	1.3	3.2	1.6	1.0
DRY RESISTIVITY AT 470 $\frac{kg}{cm^2}$ [$m\Omega\ cm$]	77	88	79	4224	51

Table 1 Carbon and Lamp Black Characteristics

To test the effects of these compounds on the behavior of a lead acid battery, full 12v, 59Ah EFBs were made and cycled at a 17.5% DoD.

In this cycling test, the battery using CB 3 showed the greatest cycle life with around 1000 cycles and the worst performing battery using CB 2 with around 230 cycles. Using this same method, a standard flooded battery typically fails after 200 cycles [35]. This particular test shows that the addition of carbon blacks positively effects the cycle life of a LABs that undergo PSoC cycling. Another test done on the carbon blacks used in this experiment, Raman spectroscopy, showed that the more ordered the structure of the carbon black as determined by a ratio of the D-band and G-band intensities, the higher cycle life its respective battery experienced [35].

In an experiment focusing on activated carbons instead of carbon blacks, 2v test cells made up of 2 positive plates and 1 negative plate with an AGM separator we built using paste mixes containing 2% weight of the activated carbons under investigation [36]. The cycling test used in this experiment initially discharged the 2V cells to 50% DoD, followed by a cycling scheme meant to imitate micro-hybrid driving. The cycles consisted of a charge step at a 2 C rate for 90 seconds with an upper voltage limit of 2.54 V, a rest step for 10 seconds, a discharge at a 2 C rate for 60 seconds, and a rest step for 10 seconds [36]. The results of this test on the reference cell, the activated carbon cells, and the activated carbon cell with graphite can be seen in Figure 5.

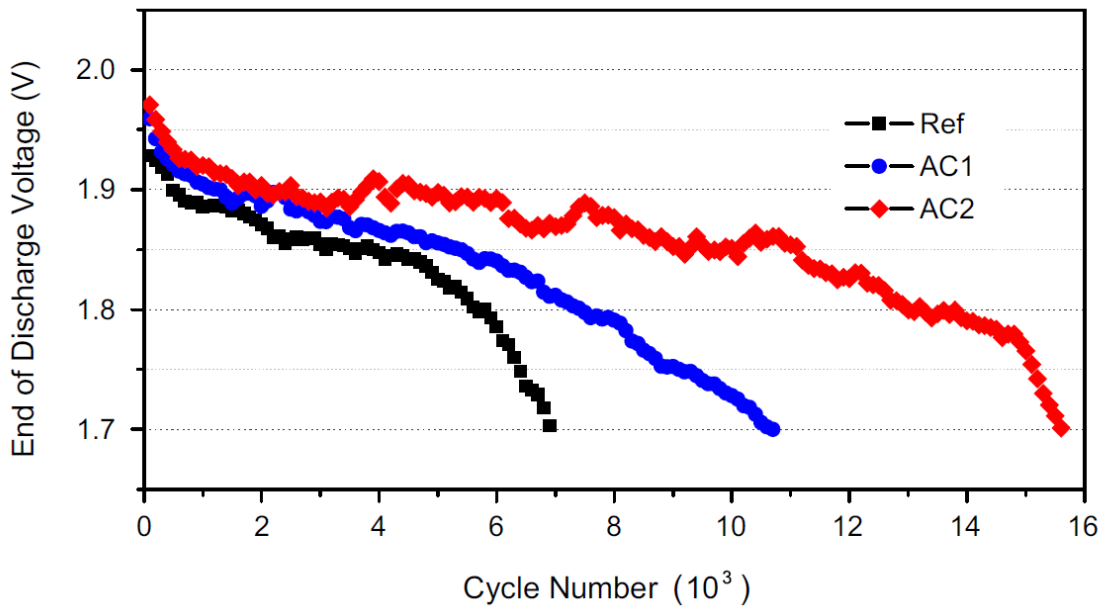

Figure 5:HRPSoC cycling on activated carbon samples [36]

Comparing the cycle life of the two activated carbon cells and the reference cell show a clear trend that, to a point, the larger particle size of the activated carbon will lead to a longer cycle life. The reference cell, with no activated carbon, experienced the shortest cycle life followed by the small particle size (4µm diameter) activated carbon, with the larger particle size

(68μm diameter) activated carbon experiencing the greatest cycle life with 7,000, 10,700 and 15,600 cycles respectively.

The role that the activated carbon plays goes deeper than simply extending the cycle life of the battery. Focusing on the larger diameter activated carbon, AC 2, highlights the benefits of using activated carbon. One major benefit of the activated carbon lies in its pore volume and size. With a volume of 1.662 $cm^3 g^{-1}$ and an average pore diameter of 2nm, the activated carbon can accommodate large amounts of H_2SO_4 [36]. The effect of this heightened acid accommodation is to provide acid to internal portions of the plate which increase the amount of the NAM that can be easily used, resulting in more surfaces for lead sulfate crystals to form, higher charge acceptance, and longer cycle life thanks to the formation of fewer large sulfate crystals. Figure 6 shows the schematic of how these large activated carbon particles act to provide acid to more of the NAM.

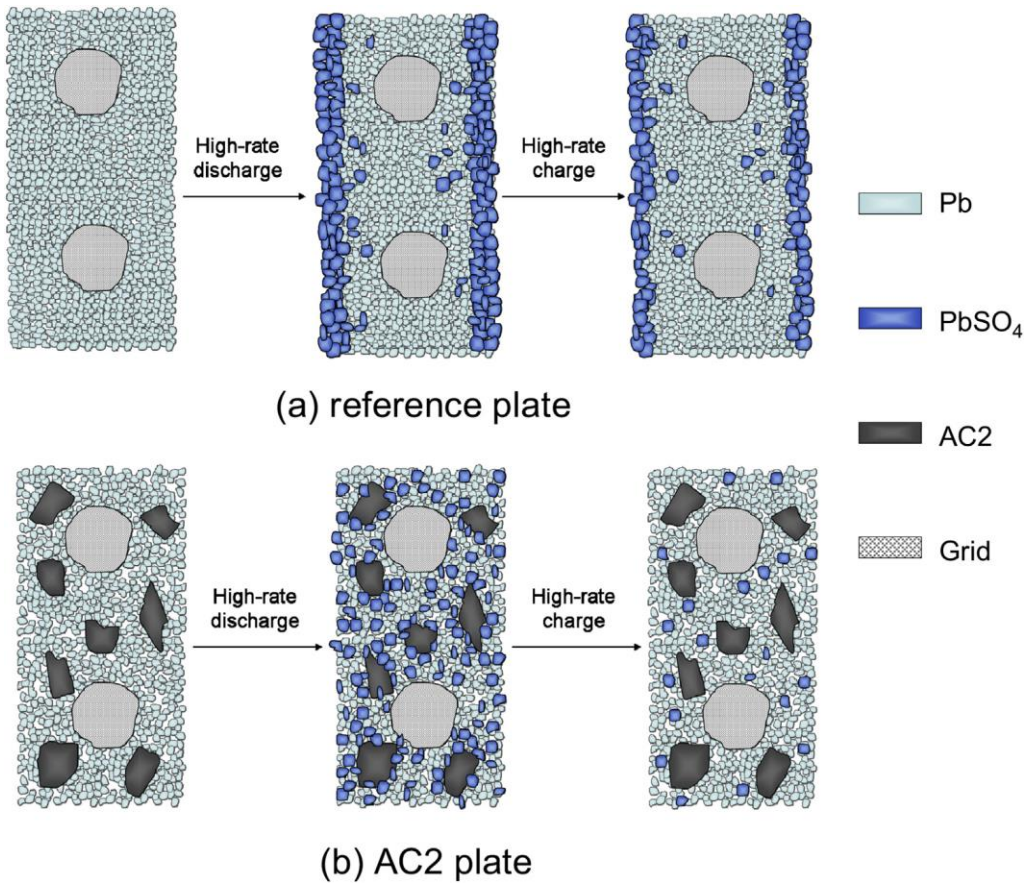

Figure 6: Carbon additive effect on HRPSoC Cycling [36]

As the diagram shows, the effects of activated carbon will be especially pronounced during high-rate discharges. This high-rate discharging behavior is common in micro-hybrid vehicles since the current needed to restart the motor after a rest cycle is both a common occurrence and requires a large, short burst of current.

1.8.2 Carbon Nano-Tubes

Another carbon additive technology that has garnered attention is the application of carbon nanotubes (CNT) to negative plate mix to improve the performance of lead acid batteries. One issue with the use of carbon additives is that increasing weight percentages of carbon can work to decrease the density of the plate mix, resulting in lower capacities for the battery. The goal then, would be to find a new carbon allotrope that is able to match the charge acceptance

and cycle life benefits of other carbons without also reducing the capacity. Carbon nanotubes may be able to provide benefits to charge acceptance and cycle life while also improving the mechanical stability of the plates [37]. One predicted benefit that the CNTs will have has been seen with other carbon additives as well; prevention of large sulfate crystal growth. By improving the electrical conductivity within the plate, combined with the conductive matrix that the nanotubes form within the active mass, lead sulfate crystal growth is dispersed throughout the negative plate [37].

In one experiment, multiwalled carbon nanotubes (MWCNT) of two separate varieties were used. In the first group, the nanotube diameter was 10-15 nm and 1-10 microns long and the second group contained nanotubes with a diameter or 40-60 nm and a 15 micron length. The weight percent of the nanotubes in the paste mixes ranged from 0.008-0.02% [37]. When testing the effect of the CNTs on the negative plates, a 2.4v cell was made using two positive plates and 1 negative plate. These cells were cycled by discharging to 30% DoD at a 0.25 C rate and charged at a 0.5 C rate. Cell failure was determined to be a voltage reading of 1.75V at 30% DoD% [37]. Tests were run on a standard flooded cell, a flooded cell with the CNT additive in the plates, and a gelled electrolyte with the CNT additive in the plates. This test showed the standard cells tend to fail at around 250 cycles where the flooded and gelled cells with the CNTs in the positive plate failed at around 450 and 750 respectively.

The addition of the CNTs has a substantial effect on the cycle life of these 2.4V cells, but the effect of size is the opposite of the activated carbon discussed in the previous section. With these commercially available MWCNTs, the longer and larger diameter CNTs showed a longer cycle life than the reference cell with no modification, but had a significantly shorter life than the cells prepared using the shorter and smaller diameter CNTs. While the exact reasoning behind

the difference in performance is not known, the initial assumption is that better mixing of the smaller CNTs lead to this result [37].

Similar work has been done using a different CNT type known as Molecular Rebar® or discreet carbon nanotubes(dCNT). Due to a proprietary preparation process these dCNTs look and behave differently than other commercially available CNTs. Instead of clustering with small aspect ratios of about 1 like the stock CNTs in Figure 7 (A), the molecular rebar disperses as a mat with aspect ratios close to 70 [38].

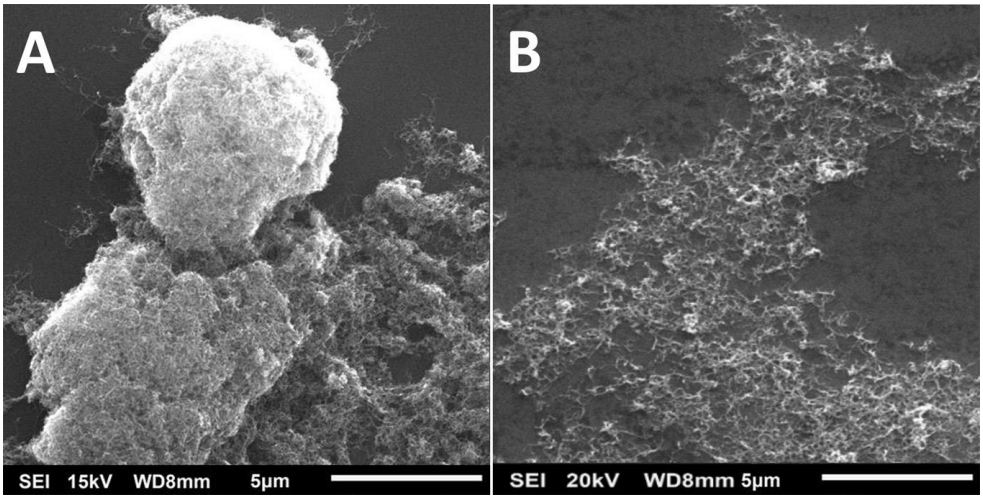

Figure 7: 5000x magnified SEM images of (A)commercially available CNTs. and (B)Molecular Rebar [38]

For the electrical testing of the effects of the dCNTs against conventional CNTs and reference cells, full batteries were built and tested to determine their behavior in a number of tests. The results are the average of five identical batteries. The two tests of interest here are the cold cranking test, where the batteries were discharged at -18˚C at 270A for 30 seconds, and the cold charge acceptance test, where the batteries were discharged to 50% DoD then cooled for 18 hours at 0˚C before a constant 14.4V recharge [38].

The result of the cold cranking tests showed that batteries with the dCNT added to the negative plates showed a 6-10%increase in the length of time needed to reach the 6V level and 2% increase in the voltage measurement after 30 seconds under the 270 A discharge. While these improvements are not large, it is noted that any improvement in cold cranking values is surprising due to the typical negative effects of carbon additives on cold cranking [38].

The cold environment charge acceptance test also showed beneficial results from the use of the dCNTs. From the DoD of 50% the batteries were charged for 10 minutes at a fixed 14.4V with variable current. Figure 8 shows the comparison of the modified and unmodified battery types. At the very beginning of the recharge step, the current levels are difficult to differentiate, but once the curves begin to level out, the dCNT battery has a definitively higher amperage being allowed into the battery. The differences between the two battery types were a 13% increase in the allowed current, and a 6% increase in the charge accepted, Ah during the 10 minutes [38].

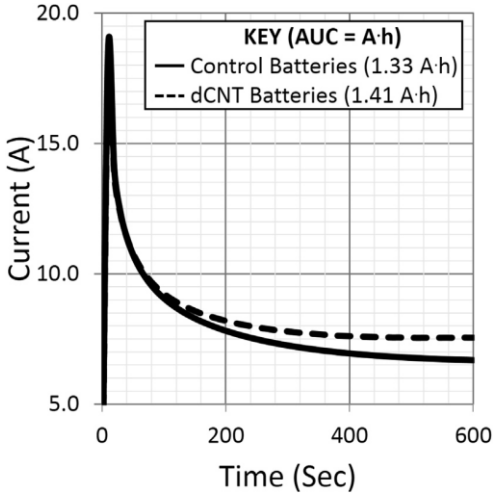

Figure 8: Cold charge acceptance test

While these discreet carbon nanotubes appear to have positive effects on the electronic behavior of the batteries without any negative effects, further research into ideal weight percentages, effects in the positive active mass, and tests under more conditions are necessary to show how truly effective this technology is.

1.8.3 Graphite

Graphite is the final form of carbon to be discussed here for use as an additive to the active mass in lead acid batteries. Graphite has a hexagonal structure and forms in layers with strong bonds within a layer and weak bonds between layers [39]. In one test, two different forms of graphite were used; expanded graphite and flake graphite. These two forms have similar conductive capabilities but have very different surface areas [40]. For comparison, a control batch using carbon black was also tested. The goal of these graphite additions is to improve the high rate partial state of charge (HRPSoC) cycling as seen in micro-hybrid applications. Through gas intrusion testing the surface area of the samples were taken and showed that the 1.5% by weight addition of expanded graphite increased the specific surface area (SSA) by 25% where the 1.5% by weight flake graphite showed a small reduction in surface area compared to the control batch containing 2% by weight carbon black [40].

Several tests were run to show the difference in the electrical effects of the new additions. The first, constant discharges at currents ranging from 10-500A showed no differences between the additives. To test the PSoC characteristics, 36V prototypes (six 6V modules in series) were tested at different depths of discharge (DoD) ranging from 0-80%. The tests showed improved charge acceptance for the expanded graphite mainly between 20-80% DoD. The samples using the flake graphite showed a reduction in charge acceptance, most likely due to the reduced SSA of the negative plates [40].

A second test was used to determine the effect these additives would have on the cycle life of the battery. Using the Power Assist Life Cycle Test from EUCAR at a 2.5% DoD [40]. Figure 9 shows the cycle used in this test.

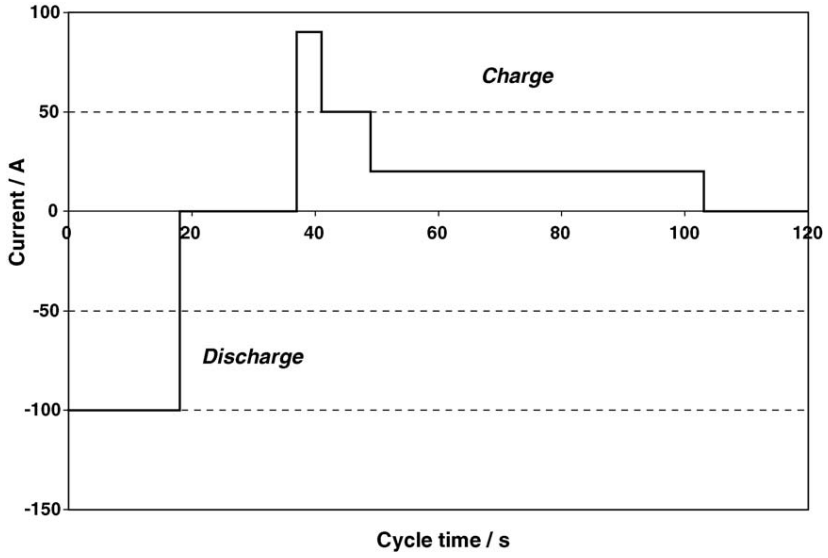

Figure 9: EUCAR Power Assist Life Cycle Test[40]

These cycles first discharge the battery to a 60% SoC before running the battery though a cycle representing those seen in hybrid electric vehicle (HEV) operation including rest, regenerative breaking, cruising, and boosting steps. To determine an end to the test, a battery must have reached either 5V during a 5C discharge or the control capacity, measured after every 10,000 cycles, fell below 50% of the original capacity. In these tests the prototype batteries using the expanded graphite showed improved values over the standard containing carbon black and a larger improvement over the prototypes using the graphite flakes. The expanded graphite prototypes showed higher end or discharge voltage (EDVs), lower increases in internal resistance after cycling, and an approximately 20% increase in cycle life over the standard prototype using the carbon black additive [40].

Carbon additives to both the positive and negative active masses of lead-acid batteries show promise for increasing the charge acceptance, capacity, and cycle life of lead acid batteries whether the additive is in the form of carbon blacks, graphite, activated carbon, or CNTs. Given the wide variety of additives available, there are also many considerations to be made to ensure a positive outcome from the addition of additives. Weight percentage, surface area, pore size, and aspect ratios all have significant effects on a carbon additive's behavior in terms of water consumption and plate strength in addition to the electronic effects [38]. While the mechanism is in some cases unclear, the positive effects of carbon additives are clearly supported and required continued research to optimize the role carbon can play in lead-acid batteries.

To conclude on carbon additives, they have the ability to increase capacity and charge acceptance, and cycle life of lead-acid batteries. The methods through which these changes occur include enhancing conductivity, encouraging the formation of small, easily dissolved $PbSO_4$ crystals, and introducing impurities that resist the hydrogen evolution [41].

1.9 Increasing Micro-Hybrid capability through Changes in Electrolyte Composition

Another viable approach for increasing the performance of lead-acid batteries is by changing the composition of the electrolyte. This field of research has not been very active in recent years with a large amount of the research in this area having been done in the 1990's and early 2000's. A major difference between todays lead-acid battery research and older research is its main goals. Older researched focused on many of the same areas as today including cold cranking performance, reducing plate sulfation, minimizing gas generation, and reducing grid corrosion. One major research area not in older experiments is dynamic charge acceptance. During the 90's the primary use for lead-acid batteries were automotive and deep cycle uses with no need for HRPSoC cycling ability. Many additives have been used to improve various

characteristics of the battery. Unfortunately, making changes to improve one attribute often effects other battery parameters.

1.9.1 Acid Additives

One grouping of additives that have been used in lead-acid batteries is other acids. Sulfuric acid is the one that gives lead-acid batteries its name, but many acids including citric, boric, and phosphoric acid have been used. Phosphoric acid was one of the earliest acids to be used as an electrolyte additive with active research beginning in the 1920's [42]. According to this early work performed by Muritz Kugal and Ing Max Rabl, the beneficial effects of adding phosphoric acid included small and dispersed lead sulfate crystals, reduced shedding of the electrodes, and no loss in capacity when added in the appropriate amount [42]. The addition of phosphoric acid was continued by the German battery company Duros, a future Varta subsidiary, until the 1970's

Jumping forward to the mid 1990's and early 2000's, phosphoric acid's effects on a lead acid battery were still being investigated. The main use of the acid is for increasing cycle life for deep discharge applications [43] [44]. The increased cycle life from phosphoric acid additions is typically attributed to the reduction of positive plate shedding and reducing positive grid corrosion [43]. The main drawback of adding phosphoric acid is the effect it has on the battery capacity. The formation and dispersion of fine lead sulfate crystals instead of large crystals, which helps increase the cycle life, also acts to reduce the capacity of the positive plate by up to 15% [44]. Given the nature of the trade off, the use of the additive can be selected when the end use of the battery prioritizes cycle life over capacity.

The effects of phosphoric acid additions have been measured using cyclic voltammetry in a study by K. Saminathan et al. 4.5M sulfruric acid with increasing concentrations of phosphoric

acid additions were cycled between 600 to 2200mV versus Hg/Hg_2SO_4 at a fixed scan rate of 50mV/s [43]. In the initial test with pure sulfuric acid there are two distinct peaks reflecting the formation of α-PbO_2 and β-PbO_2 with the positive plate consisting of a lead-tin alloy. As the concentration of the phosphoric acid was increased, the peak current for the α-PbO_2 was steadily reduced and the β-PbO_2 peak dramatically reduced and disappears at higher the higher phosphoric acid combinations. These results were also seen to a large extent in positive plates consisting of a lead-calcium-tin alloy. In addition to the inhibited formation of β-PbO_2, the increasing phosphoric acid concentrations also lead to a positive shift in the oxygen evolution potential[43]. In all, phosphoric acid additions have multiple effects on lead acid batteries including increased deep-cycle life, lowered capacity, reduced β-PbO_2 formation, and reduced oxygen formation.

Acid additives have also been used to reduce the self-discharge process in lead-acid batteries. Reducing self-discharge is typically done by inhibiting the reaction of the lead oxide to lead sulfate while the battery is not in use. Boric acid is thought to reduce the self-discharge process by modifying the physical structure of the PbO_2 crystals and delays the formation of $PbSO_4$. The result of adding boric acid was a reduction in the voltage drop from 0.01 $\frac{V}{day}$ to 0.0025 $\frac{V}{day}$ when compared to a standard battery with a pure sulfuric acid electrolyte [45].

Similarly, stearic acid causes a 50% reduction in self-discharge voltage of 0.005$\frac{V}{day}$. In contrast with the boric acid, stearic acid is a surfactant that is absorbed into the surface of the plate and decreases the three-dimensional growth and increases the two-dimensional growth of the PbO_2. This PbO_2 layer is more difficult to reduce to $PbSO_4$ than one that is formed in pure sulfuric acid[45]. Citric acid has also been used as an additive, but while the self-discharge rate

is reduced by 25% to 0.0075$\frac{V}{day}$, the overvoltage for both the oxygen and hydrogen evolution reactions is reduced, leading to increased gassing rates [45].

1.9.2 Sodium additives

Sodium sulfate is a compound that is already commonly used as an electrolyte additive for lead-acid batteries. Since at least the 1970's sodium sulfate was seen as a cost effective additive over other sulfate salts including potassium, lithium, magnesium, cadmium, zinc and aluminum to reduce the solubility of lead and help prevent shorts [46]. As mentioned with other additives, typically multiple aspects of battery performance are changed and sodium sulfate is no different. A number of studies have been done looking at sodium sulfates effects on a range of parameters including hydrogen evolution, anodic passivation [47], capacity, cold cranking, and charge acceptance [48].

For these tests, a standard sulfuric acid solution was prepared with no sodium sulfate, then acid solutions with increasing levels of sodium were sulfate were made and tested to show the effects of the changing sodium sulfate concentrations. One set of tests out of China looked specifically at the sodium sulfates effects on hydrogen evolution and anodic passivation. Using linear sweep voltammetry(LSV) the hydrogen evolution decreased from the 3.5 mol/L sulfuric acid solution to the 3.5 mol/L sulfuric acid solution with 0.05 mol/L of sodium sulfate. However, the trend shows that with increasing amounts of sodium sulfate from 0.05 mol/L to 0.5 mol/L the cathodic currents related to hydrogen evolution increases [47]. To summarize, at low levels sodium sulfate acts to reduce the hydrogen generation, but at higher levels it works to increase hydrogen generation. Using the same solutions and a cyclic voltammetry (CV) test, the

same group concluded that adding sodium sulfate inhibits the growth of a PbO film on the lead grids resulting in less corrosion and better conductivity [47].

Another way to investigate the additive effects are through cycling of larger prototype batteries instead of sample electrodes to better represent what the practical changes the additive causes. This approach was used to investigate varying sodium sulfate concentrations on capacity, cold cranking, and charge acceptance, and high rate discharge following Japanese Industrial Standards(JIS) D 5301 for lead acid batteries[48][16] . For these tests flooded 12V, 65Ah batteries with 8 positive and 7 negative plates were used. The sulfuric acid contained weight percent amounts of sodium sulfate of 0%, 0.5%, 0.75%, 1.0%, 2.0%, 4.0%,6.0%, 8.0% and 10.0% [48]. In a capacity test, the batteries were discharged at a 5C rate and showed a mildly decreasing trend in capacity as the sodium sulfate concentration grew. For cold cranking, the batteries were discharged at a high rate (specific current used not given) and the voltage was taken after 30 seconds. The trend in this test showed increasing voltage at 30 seconds up to 0.75% weight sodium sulfate followed by steady decrease of voltage with increased concentrations.

The test for high rate discharge used batteries soaked at -15°C and discharged them at a high rate (likely 150A [49]). The voltage was measured after 5 seconds of discharge as was the total time needed to reach 6V [48]. The data showed that the 5second voltage was highest at 1% sodium sulfate by weight and that adding increasing amounts passed 1% resulted in decreasing voltage. The time to reach 6V, however, showed a much different trend. Here, a linear relationship was formed with increase time throughout the samples with the no sodium sulfate standard falling between the 4% and 6% samples.

The final test, charge acceptance, is the most interesting test when considering micro-hybrid use. For this test, the batteries were soaked at 0°C for 12 hours before charging at a constant 14.4V. The current measurement was taken at the 10^{th} minute[48] [49]. The results showed that the charge acceptance was highest at low to no sodium sulfate and decrease dramatically upon increasing the sodium sulfate concentration. From these tests, the addition of sodium sulfate shows mainly negative impacts on the electrical behavior of the lead acid battery.

To summarize, the addition of sodium sulfate to lead acid batteries has been a common practice for decades. As the previous tests have shown, its impacts on the electrical performance of the batteries is generally negative. As mentioned earlier, the primary use of sulfate salts, and sodium sulfate has been to help prevent shorting from occurring [46]. Sulfate salts, and sodium sulfate in particular, are used to reduce the solubility of lead sulfate and limit the free lead ions in the acid that lead to shorts. This is achieved through the common ion effect, where the excess of SO_4^- ions in the electrolyte from the sodium sulfate shift the equilibrium closer to the solid lead sulfate crystals [50]. In AGM batteries this is particularly useful as lead sulfate is more likely to precipitate in regions of low acidity common in the separator during deep discharges when the overall pH of the electrolyte is lower. Upon recharging, the sulfate will be driven back into the solution but metallic lead can be left behind in the separator eventually leading to dendrite shorts through the separator [51]. Given that the demands have changed for batteries over the years and that for micro-hybrid applications charge acceptance is a very important parameter, new additives are needed that can fulfill the role played by sodium sulfate without the negative impacts on the batteries electrical behavior.

An interesting new additive sharing a sodium salt based chelating agent Na_2-EDTA. Chelating agents form two or more coordinate bonds between a polydentate ligand and a central

atom, typically a metal ion. In this reaction, the Na_2-EDTA molecule bonds with lead sulfate, expelling the sulfate ion by the mechanism shown below.

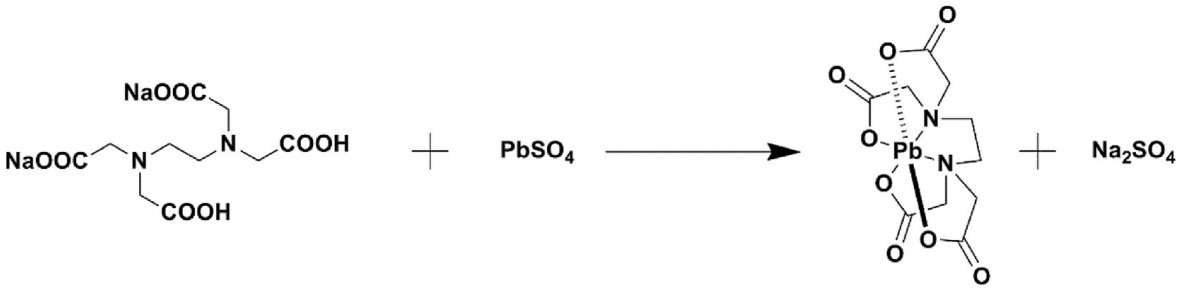

Figure 10:Chelating additive Na_2EDTA mechanism with lead sulfate.[52]

In order to test the effects this compound would have on lead-acid battery operation, 2V 2.8Ah cells were made using a two negative plates and one positive plate, an AGM separator, and 4.5M sulfuric acid with additions of 0%,0.25%, 0.5%, 1% by weight [52]. Further information on cell design are available in the literature. The tests conducted to evaluate changes in electrical behavior included galvanostatic charge-discharge studies, I-V characteristics, impedance, and cyclic voltammetery [52].

After initial capacity tests were completed the 0.5% Na_2-EDTA electrolyte showed the highest capacity and was used as the only electrolyte for comparison with the standard sulfuric acid electrolyte [52]. In the initial C/20 capacity tests showed the 0.5% Na_2-EDTA electrolyte had a capacity of 3.3Ah hours compared to the 2.8Ah of the standard electrolyte. Rate capabilities for these two electrolyte were also tested in terms of discharge capacity(Ah) with the 0.5% Na_2-EDTA electrolyte showing around 10% improvements at low C rates (C/20 and C/5) and over 20% improvements at high C rates (3C). These results were attributed to the increased

mobility of ions from the electrolyte to the plates due to a decreased non-conductive lead sulfate layer on the positive plate [52].

In addition to increased rate performance, the 0.5% Na_2-EDTA electrolyte also showed greater cycling performance as capacity was maintain after 135 deep discharge cycles when the standard cells began seeing decreasing capacity after 80 cycles. Along with improved cycle life, the Na_2-EDTA electrolyte also showed a reduction in the in ohmic resistance throughout the various the entire range of charge states. From this observation the conclusion drawn was that the Na_2-EDTA was decreasing sulfation and in doing so decreasing resistance [52].

1.9.3 Surfactant Additives

Another electrolyte additive for improving the lead-acid battery electrolyte is a surfactant. A surfactant, also known as a surface active agent, is a compound that reduces surface tension and increases wetting characteristics [53]. Surfactants have been used in other battery technologies to improve performance by reducing hydrogen formation, limiting metal corrosion, and modifying crystal morphology [54]. The surfactants, which are comprised of a long hydrophobic chain with a hydrophilic end, are absorbed into the hydrophobic electrode and change the characteristics of the interface of the electrode and electrolyte [54]. It is also important to note that the behavior of surfactants varies significantly from factors including the charge of the end group, positive or negative, and the concentration of the surfactant, and how well it is absorbed into the plate surface [54].

Interest in surfactants date back to at least the 1950's when a patent for perfluoroalkylsulfonates was filed claiming that their addition increased wetting of the electrodes, increased surface area by decreasing crystal size, reduced water loss from evaporation, and sequestered impurities in the electrolyte from additions of water[55]. In

addition to US patents, several patents for similar surfactant additives were made in Japan in the early 1990's[56]. In a study performed in 1998, several different perfluorinated surfactants with anionic, cationic, and non-ionic end groups were used to increase the utilization of the positive active material in lead acid batteries[56]. The results of these tests were not positive due to additives breaking down or from shortened cycle life attributed to a loss of grid contact in the positive plate[56].

In a recent study by Ghavami et al four surfactants, cationic cetyl trimethyl ammonium bromide (CTAB), cationic cetyl trimethyl ammonium bromide (CTAB), sodium dodecyl sulfate(SDS), and nonionic t-octyl phenoxy poly ethoxy ethanol (Triton X-100), were used to observe the effects they have on the negative active mass (NAM) and the effects were evaluated using electrochemical impedance spectroscopy (EIS), cyclic voltammetry (CV), scanning electron microscopy (SEM), and X-ray diffraction (XRD).

	SURFACTANT TYPE	CONC. (PPM)	MOLECULAR WEIGHT	CRITICAL MICELLE CONC. ($\boldsymbol{mM}$)	CHEMICAL FORMULA
CTAB	Cationic	50	364.45	1	$C_{19}H_{42}BrN$
SDBS	Anionic	50	348.48	1.6	$C_{18}H_{29}NaO_3S$
SDS	Anionic	50	288.37	8	$NaC_{12}H_{25}SO_4$
TRITON X-100	Non-ionic	50	647	0.22-0.224	$C_{14}H_{22}O(C_2H_4O)_n$

Table 2:Surfactant properties.

For testing flooded cells with a 2.1 Ah nominal capacity were used with further cell design details in the literature [57]. The surfactants were added to the electrolyte after the cells went through formation and kept under 50 ppm to prevent the formation of micelles in the

electrolyte. The cells were tested for capacity though full discharges and in PSoC mode using the method shown in Figure 11 below.

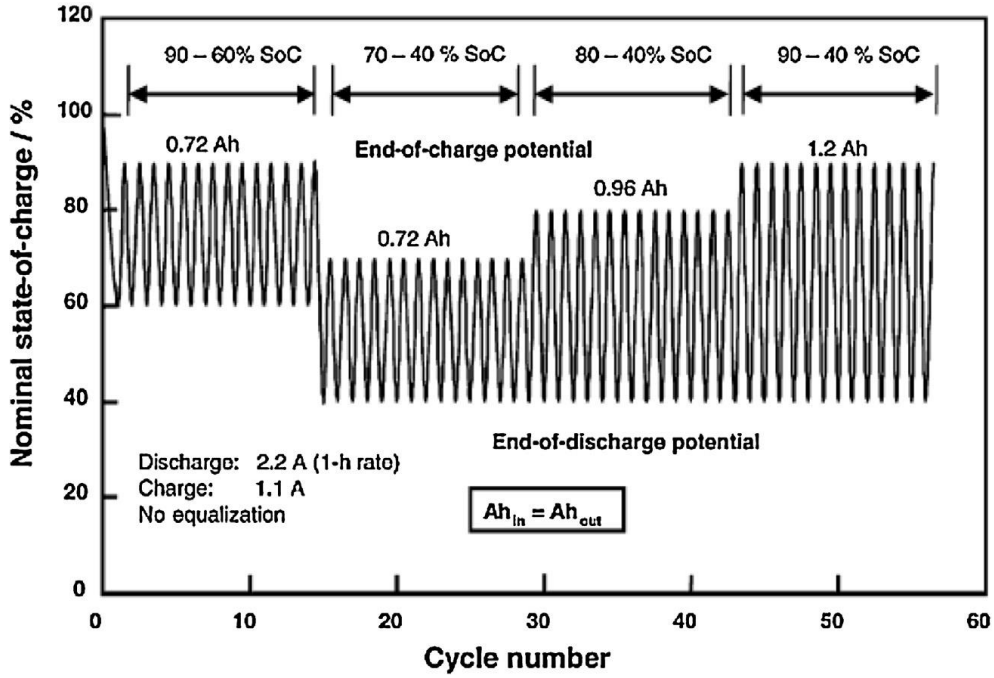

Figure 11:PSoC cycling profile.

The pattern of the end-of-discharge potential (EoDP) and end-of-charge potential (EoCP) were used to examine the effects of the additives during the PSoC cycling where the output and input charge are equal, resulting in consistent under charging [54]. To evaluate the charge efficiency of the cells during the PSoC cycling a conversion indicator calculated by ratio of the charge input and the discharge capacity of the previous step.

In terms of capacity, the SDBS electrolyte had the best capacity values around 2.4 Ah, with the SDS and TX-100 at around 2.3 Ah. The standard electrolyte mixture's capacity was about 2 Ah with the CTAB very close behind. The PSoC cycle testing gives a good look at how the cells would operate in a micro-hybrid environment. Figure 12 below shows the each of the cells performed in the PSoC testing.

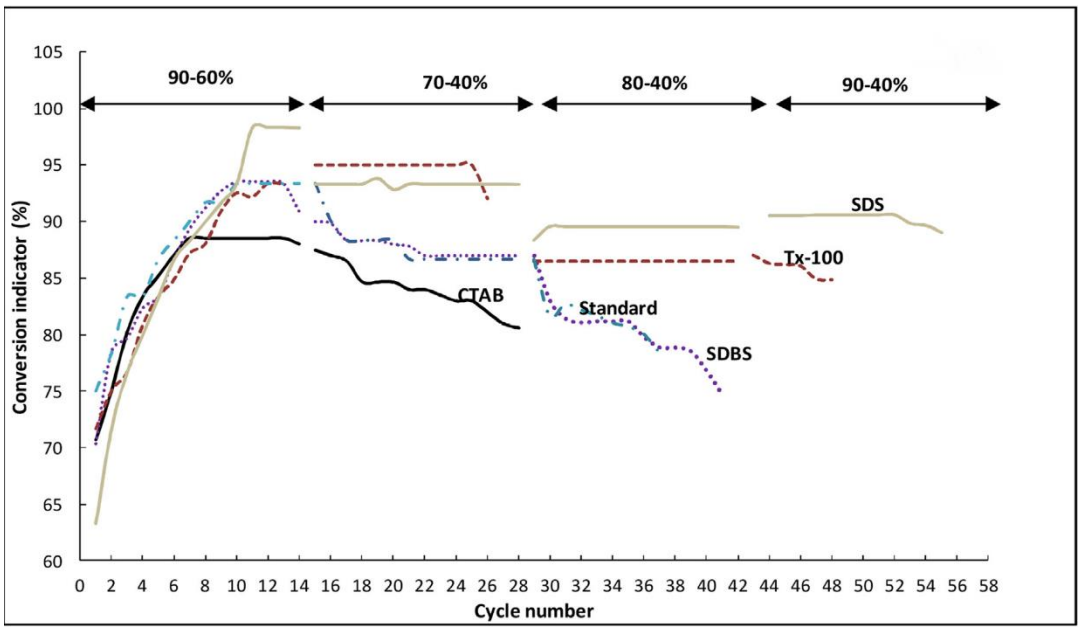

Figure 12: Conversion indicator performance under PSoC cycling.

From the plot, the SDS electrolyte showed the longest cycle life in this test and also had the greatest energy efficiency in three of the four SoC windows. The standard performed worse than both the SDS and Tx-100 electrolytes and failed to make it into the last cycling window. The CTAB electrolyte performed far worse than the rest of the field with substantially lower energy efficiency and the worst cycle life.

The SEM analysis of the plates after testing also shows a critical element in the differences in the electrical behavior of the cells. The impact the different surfactants have on the shape, size, and dispersion of the lead sulfate crystals correlates strongly with the charge acceptance and cycle life of the batteries in this test. The best performing surfactant additive, SDS, showed fine and well dispersed crystals on the negative plate. The worst performing surfactant additive, CTAB, Showed large and course needle shaped crystals [54]. This same type of crystal growth is commonly associated with dendritic shorts.

In Summary, certain surfactant compounds can increase certain parameters of lead acid batteries while others either limit certain behaviors of break down in the highly oxidative environment found in lead acid batteries.

1.9.4 Ionic Liquid Additives

Another contender in the realm of lead acid battery electrolyte additive is ionic liquids. A common definition of ionic liquids is a salt compound that is a liquid below 100°C [58]. This is a very broad definition that covers a wide range of organic cations including quaternary ammonium cations, heterocyclic aromatic compounds, and pyrrolidinium cations combined with an equally wide range of anion [59]. Given the variability of possible of an ionic liquid's makeup, the resulting properties can vary greatly. The characteristics that make these compounds desirable for battery electrolytes, as seen by their heavy use in lithium ion batteries[59]. The characteristics these materials have that are so appealing for electrochemical applications include their liquid state at room temperature, nonflammability, high ion density, thermal stability, wide electrochemical windows and their highly customizable nature [59].

In 2009 some of the first tests were run specifically on the effect that ionic liquids could have on a lead acid battery as an additive to the electrolyte. The four ionic liquids, triethyl ammonium hydrogen sulfate, dibutyl ammonium hydrogen sulfate, benzyl ammonium hydrogen sulfate, and 1-butyl-3-methylimidazolium hydrogen [59]. The ionic liquids were added to 4.0 mol/dm^3 sulfuric acid in the amounts of 2.5, 5.0, 10.0, 15.0 and 20.0mg/cm^3 and tested using cyclic voltammetry between 2.500V to +2.500V at a sweep rate 50.0mV/s. Electrode specifications may be found in the literature [59].

Using cyclic voltammetry and SEM analysis several trends were seen resulting from the addition of the ionic salts. First, these additives increased both the hydrogen and oxygen

overpotentials which should lead to a decrease in water consumption. Second, the additives increased the conversion rate of $PbSO_4$ to Pb and of Pb to $PbSO_4$, which increased the utilization of the positive active material. The third and final trend established in the research was an increase in the grid corrosion.

1.9.5 Metal Ion additives

So far, most of the testing that has been done using metal ion sulfates, like sodium sulfate, has been done to establish the effects the salts have on reducing the appearance of shorts [46][50]. The prevention of shorts is caused by the reduced lead sulfate solubility caused by the increased sulfate ion concentration in the electrolyte from the added sulfate salt. The effects of the metal ions in the solution are not as well understood, especially in the role they may play in charge acceptance. The following work looks to focus on the effect that different sulfate salts will have on mainly the charge acceptance behavior of the cells, but will also consider its effects on capacity and cold cranking.

2 Experimental

The goal of the following experiments is to evaluate the impact of single metal-sulfate additives to the electrolyte of AGM lead-acid batteries using a single cell design that closely replicates a commercially made AGM battery. To accomplish this, positive and negative plates typically used in mass-market AGM batteries were used. The "battery box" is a custom designed box that allows for single cell AGM configurations, vacuum acid filling, use of pressure release valves, and thermocouple and electrode measurements. For this set of tests, the 2V, 10Ah cells were comprised of two negative plates and one positive plate, and Dumas separator

2.1 Methods and Materials

2.1.1 Acids

The standard acid used in lead acid batteries is sulfuric acid with a density ranging from 1.200 -1.300 $\frac{g}{mL}$. For these tests the stock acid solution was purchased from Alchemix and was sulfuric acid with a density of 1.24 $\frac{g}{mL}$. The standard acid for these experiments will be a sulfuric acid with sodium sulfate added at a concentration of 15 $\frac{g}{L}$. This concentration is one that is currently used as a standard concentration to produce some lead-acid batteries. By using the formula in Figure 13 below, the number of moles of the sodium ion was calculated. The concentration of other sulfate salts will be based on the equivalent amount of metal ions.

$$Mols\ Na^+ = 15g\ Na_2SO_4 \times \frac{2\ mol\ Na}{142.04g} = 0.2112\ \frac{mol}{L}\ Na^+$$

Figure 13-Sodium Ion Concentration

Using the ion concentration found in Figure 4, acids were made using 10 sulfate salts to be used in the first round of testing. Table 2 below shows the 15g sodium sulfate metal ion equivalent acids and their properties. At the .02112 M level the copper, bismuth, and tin sulfates

were over their saturation point in the acid. These acids were vacuum filtered to remove solid particles leaving a saturated solution.

	A	B	C	D	E	F	G	H	I	J
SALT FORMULA	Na_2SO_4	$MgSO_4$	$Al_2(SO_4)_3$	Li_2SO_4	$ZnSO_4$	$In_2(SO_4)_3$	$CuSO_4$	$Bi_2(SO_4)_3$	$SnSO_4$	K_2SO_4
MOLECULAR WEIGHT	142.04	120.37	342.15	109.94	161.47	517.81	159.61	706.13	214.77	174.26
SALT MASS (G)	15.00	25.42	36.13	11.61	37.90	54.68	33.71	74.57	45.36	18.40
ION CONC. ($\frac{mol}{L}$)	0.2112	0.2112	0.2112	0.2112	0.2112	0.2112	0.2112	0.2112	0.2112	0.2112
ACID DENSITY ($\frac{g}{L}$)	1.25	1.27	1.28	1.25	1.28	1.29	x	x	x	1.29

Table 3:Table of Sulfate Salt and Acid Properties. The table shows the properties for acids containing (A) Sodium Sulfate, (B) Magnesium Sulfate, (C) Aluminum Sulfate, (D) Lithium Sulfate, (E) Zinc Sulfate, (F) Indium Sulfate, (G) Copper Sulfate, (H) Bismuth Sulfate, (I) Tin Sulfate, and (J) Potassium Sulfate.

The second round of testing focused on the ions that had the best charge acceptance behavior (excluding indium sulfate) and used decreasing concentrations to establish a relationship between the charge acceptance behavior and the concentration of the metal ion in the acid. The additives that showed the best behavior at this concentration were zinc sulfate and aluminum sulfate. Tables 4 and 5 below shows the concentrations of the metal ions and properties of these additives.

ZINC SULFATE

SULFURIC ACIDS

ION CONC. ($\frac{mol}{L}$)	0.2112	0.1408	0.0704	.0422	.0387	0.0352	.0317	.0282	.0142	.0071
SALT MASS (G)	37.90	25.27	12.63	7.58	6.95	6.32	5.69	5.05	2.54	1.27
SODIUM MASS EQUIVALENT (G)	15.00	10.00	5.00	3.00	2.75	2.5	2.25	2.00	1.01	0.50
DENSITY ($\frac{g}{mL}$)	1.28	1.27	1.25	1.25	1.25	1.25	1.25	1.25	1.24	1.24

Table 4: Properties of Zinc Sulfate-Sulfuric Acid Solutions

ALUMINUM SULFATE SULFURIC ACIDS

ION CONC. ($\frac{mol}{L}$)	0.2112	0.1408	0.0704	0.0352	.0142	.0071
SALT MASS (G)	36.13	24.09	12.04	6.02	2.42	.061
SODIUM MASS EQUIVALENT(G)	15.00	10.00	5.00	2.5	1.01	0.50
DENSITY ($\frac{g}{L}$)	1.28	1.26	1.25	1.25	1.24	1.24

Table 5: Properties of Aluminum Sulfate-Sulfuric Acid Solutions

The final round of testing single metal ion additives looked at the original sulfate salts with metal ion concentrations of 0.0352 M. Table 6 shows the properties of the acids with the sulfate salt additives at the optimal concentration. At the 0.0352 M level, Bismuth was still over the saturation point.

SALT PROPERTIES	**A**	**B**	**C**	**D**	**E**	**F**	**G**	**H**	**I**
SALT FORMULA	$MgSO_4$	$Al_2(SO_4)_3$	Li_2SO_4	$ZnSO_4$	$In_2(SO_4)_3$	$CuSO_4$	$Bi_2(SO_4)_3$	$SnSO_4$	K_2SO_4
MOLECULAR WEIGHT	120.37	342.15	109.94	161.47	517.81	159.61	706.13	214.77	174.26
SALT MASS (G)	4.24	6.02	1.94	6.32	9.11	5.62	12.43(SAT)	7.56	3.07
CONC. ($\frac{mol}{L}$)	0.0352	0.0352	0.0352	0.0352	0.0352	0.0352	0.0352	0.0352	0.0352
ACID DENSITY ($\frac{g}{mL}$)	1.24	1.25	1.24	1.25	1.25	1.25	x	1.25	1.24

Table 6:Acid properties at low levels of metal ion additives. (A) Magnesium Sulfate, (B) Aluminum Sulfate, (C) Lithium Sulfate, (D) Zinc Sulfate, (E) Indium Sulfate, (F) Copper Sulfate, (G) Bismuth Sulfate, (H) Tin Sulfate, and (I) Potassium Sulfate.

2.1.2 Cell Assembly

A custom designed battery test box comprised of a main box with a cavity for plates and acid and a faceplate that is bolted onto the box once the plate stack is inside. The depth of the cavity allows for variation in the compression of the separator by changing the thickness of plastic shims in the cavity. For these tests, the target separator thickness was between 0.85-0.90 mm. Once the box has been assembled, a vacuum is applied to the box through a valve located on the top of the box. A second valve located on the back of the box allows for the acid to be pulled into the box. The acid is applied in two steps. First, 70 mL of acid is pulled into the box

followed by three “massage” pulses. Each pulse consists of pulling a vacuum (typically around 11 PSI), sealing the box, then opening the acid valve to release the vacuum. The second step is a 25 mL of acid addition. Once the box has been filled and weighed it is hooked up to an Arbin channel to begin formation. Figure 14 shows the cell during several steps of the assembly process.

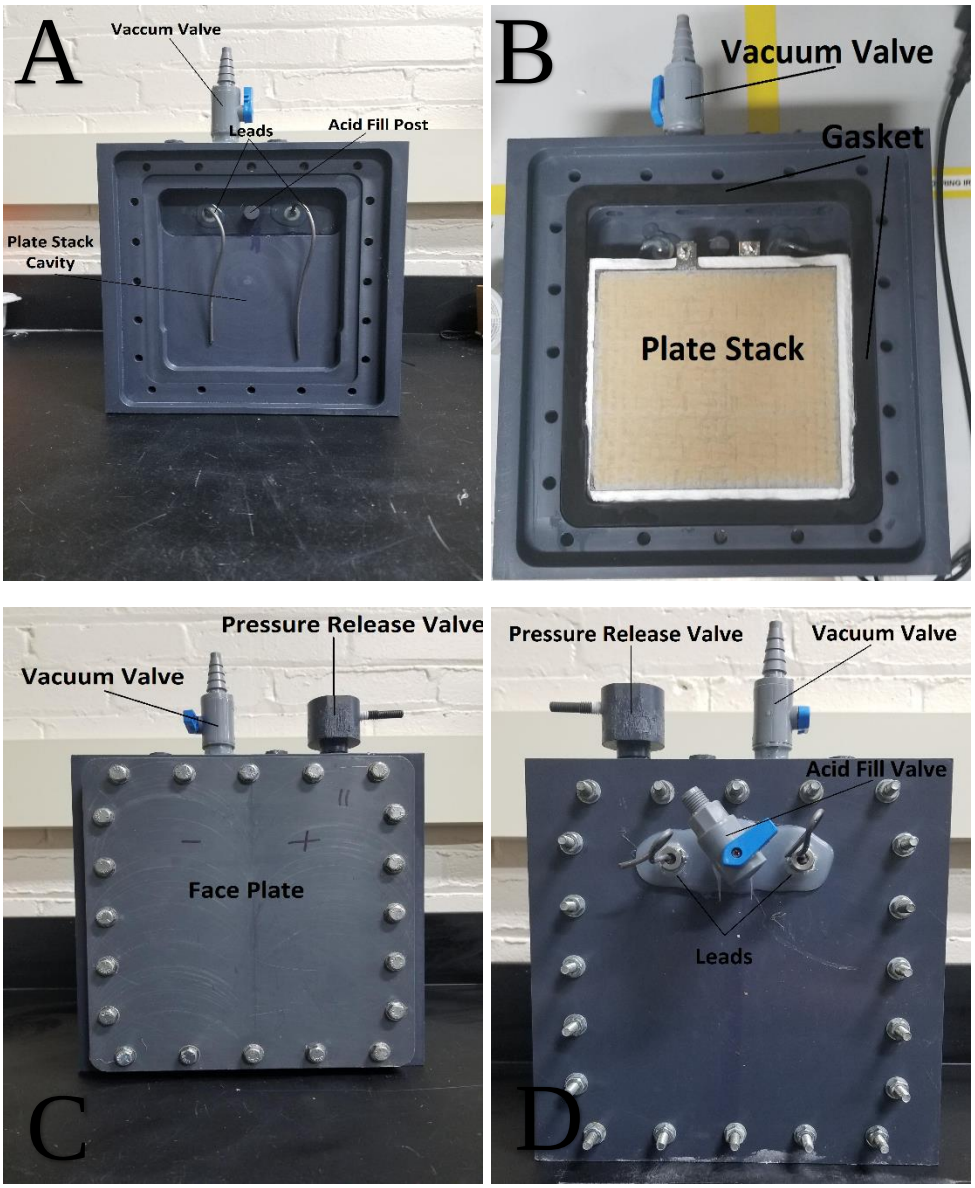

Figure 14: *Single cell construction. A) Empty battery box. B) Battery box with plate stack. C) Completed box front. D) Completed box back.*

2.2 Electrical Tests

2.2.1 Formation

When the positive and negative plates for lead-acid batteries are made, they both begin from a similar leady oxide paste mix. The main differences come from the additives to each plate, mainly that lignosulfate expanders, barium sulfate, and other additives are added to the negative mix before the paste is applied to the grids [50]. The formation process, or the initial

charge, is responsible for changing the positive and negative plates, which have the same combination of bivalent lead compounds into the lead oxide (PbO_2) positive plate and the lead (Pb) negative plate required for the electrochemical reaction to occur [50]. The formation process used for the cells in these tests is a combination of charging and rest steps over a period of 24 hours using an Arbin Instruments BT2000 to perform test cycle. Figure 15 shows the formation process.

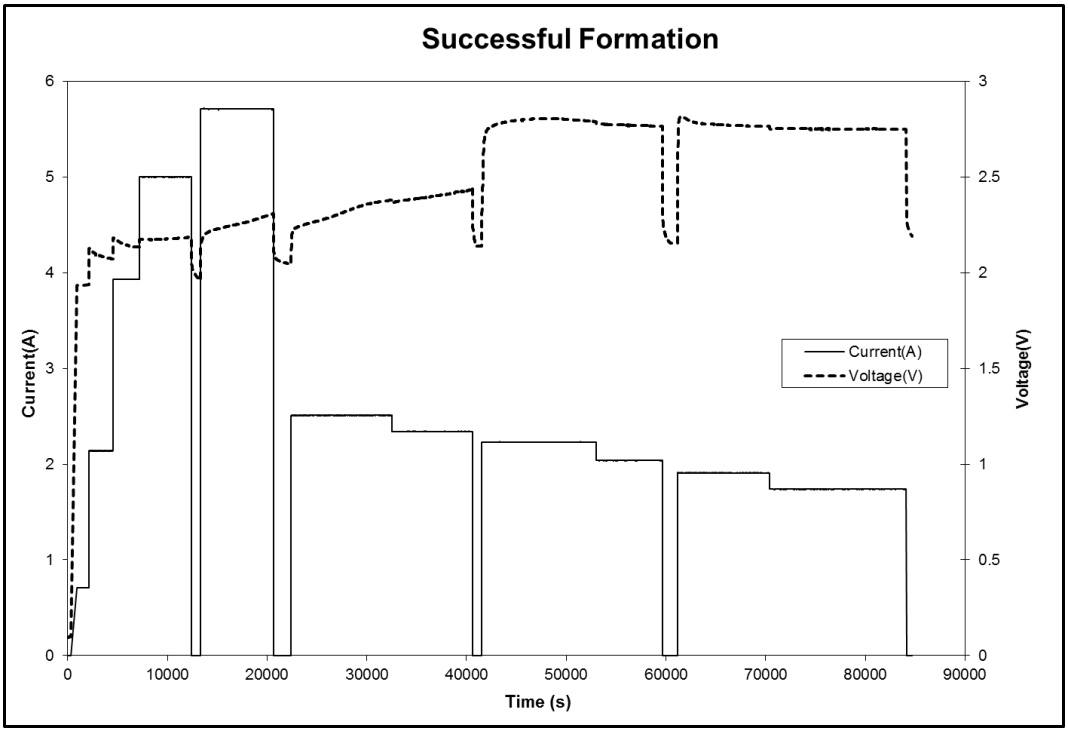

Figure 15:AGM Lead-Acid Battery Formation Plot

During the battery formation large amounts of gas generation is typically experienced. For the batteries in this test the weight loss due to gas generation is typically between 10 and 13 grams. Much of this gassing occurs during the final three charging steps when the voltage exceeds 2.5V. A good indicator for a poor or incomplete formation in these batteries can be seen by the combination of low weight loss and the voltage never exceeding 2.3V-2.5V during the

final stages of the formation charging schedule. Figure 16 shows what the voltage output looks like for a battery that fails the formation process.

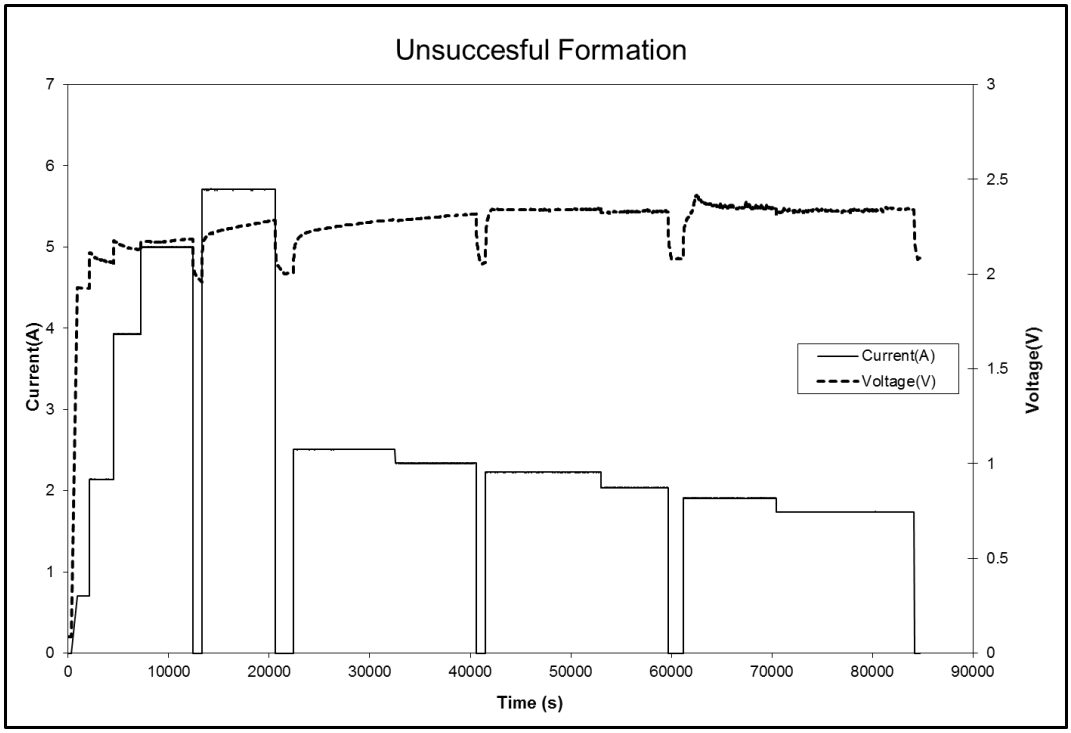

Figure 16:Failed Lead-Acid Battery Formation

2.2.2 5 Cycle-Test

The five-cycle test run on the batteries for this experiment implemented a custom schedule and an Arbin Instruments BT2000. This test is broken up into two main sections. The first section establishes the condition of the battery. After a battery has successfully completed formation it goes through four full discharge and recharge cycles. The battery is discharged at a C/5 rate (2A) for these batteries, and is recharged at a C/10 rate (1A) for these batteries, until the discharge capacity has been reached followed by some additional charging to make up for low charging efficiency. During these conditioning cycles the general capacity of the cells can be seen and is usually stabilized after these cycles. The second portion of the five-cycle test is designed to check the charge acceptance behavior of the batteries at several different SoCs.

After the final conditioning cycle the battery is discharged by 1 Ah down to a 90% SoC. After the 10% discharge the cells are rested for 12 hours before beginning the charge acceptance step. During the charge acceptance step the voltage is held constant at 2.4V and the current is limited by the charge acceptance of the battery. After 10 seconds the battery is discharged by the same amount of Ah it received during the DCA step and then another 1Ah down to an approximately 80% SoC. The same method is used to determine the charge acceptance characteristics at 80%, 70%, and 60% SoC as at 90% SoC. After the 60% SoC step the battery is fully recharged and then discharged at a C/20 rate, which is 0.5A for these batteries. Figure 17 below shows the graphical representation of the five-cycle test.

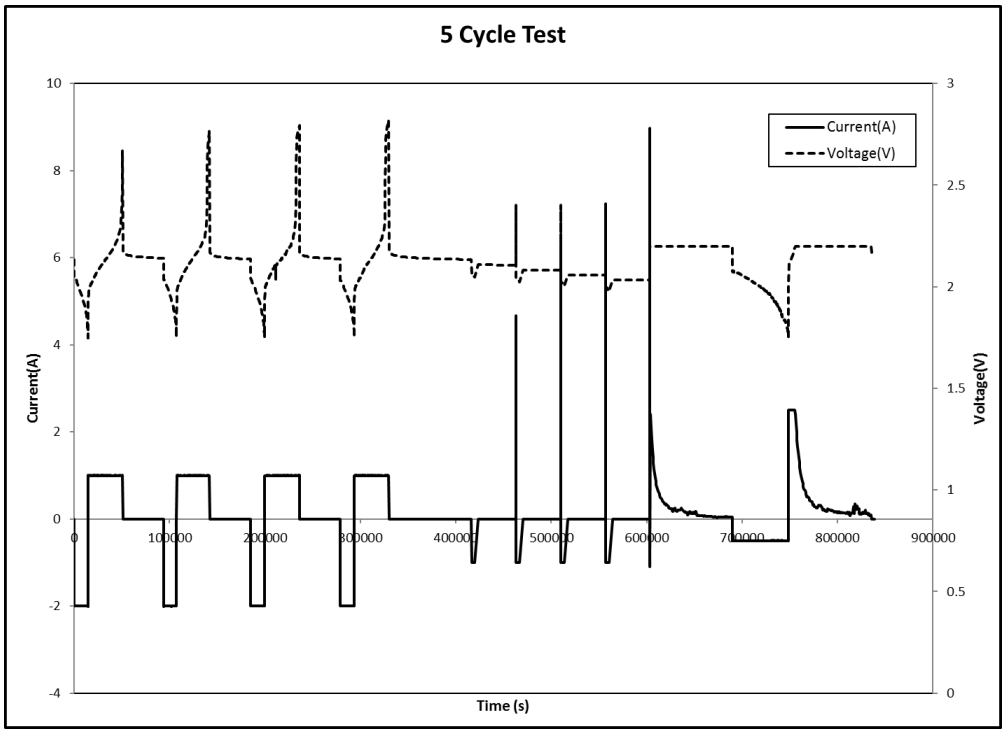

Figure 17:5 Cycle Test

Looking at the plot between 4000 and 7000 seconds the expected DCA behavior of increasing charge acceptance with decreasing state of charge can be seen.

2.2.3 Cold Cranking

One of the most important properties of lead acid batteries is their ability to operate in very cold temperatures. To determine if changes in charge acceptance came with changes in cold cranking ability, the cold cranking test for these cells is a 30A discharge on cells after completing the five-cycle test and soaking in a temperature controlled chamber at -18°C for 24 hours. The test is run until the voltage of the battery reaches 1V. The time and discharge capacity are measured using an Arbin Instruments BT2000.

2.3 Analytical Tests

2.3.1 ICP-OES

For the ICP samples, the same negative plates were used as those for the SEM/EDS samples. Sections of the lead plate were removed from all 5 positions of the plate. 5 grams of the plate were removed ground and mixed into a fine powder with a mortar and pestle. 0.25 grams of the powder were dissolved in 8mL of concentrated nitric acid (70%) and heated. After about 5 minutes 20mL of DI water was added to the solution and heating continued until the samples were completely dissolved. The solution was then transferred into a 50mL volumetric flask and diluted to the 50mL mark with DI water.

Samples were also taken from the electrolyte to help identify how the added ions are working to affect the electrical properties of the battery. Fresh electrolyte was taken for ICP testing as well as used electrolyte after the boxes had undergone formation and four conditioning cycles comprised of a C/5 discharge and a C/10 recharge. These battery boxes were broken down and the separators were squeezed to remove the electrolyte contained within. After removal from the separator, the electrolyte was syringe filtered to remove any fiberglass or other contaminants.

A PerkinElmer Optima ICP-OES machine was used for analysis. This machine uses a dual echelle monochromator with 79 lines/mm and a blaze angle of 63.4° and a dual, backside-illuminated, cooled, CCD detector. This machine uses the inductively coupled plasma to excite the components contained in the sample. Upon relaxing back to their original state, some characteristic light spectra are emitted and gathered by the optical sensor. When the target elements in the sample are in an appropriate concentration range for the sensor, the intensity of the spectra can be used to evaluate the concentration of the target elements in the solution. For these samples, the electrolytes were diluted by a factor of 300 and the dissolved plates were dissolved by a factor of 50 for evaluation.

2.3.2 SEM/EDS

After being run through the formation test, boxes that contained Aluminum and Zinc acids at the 15g sodium sulfate equivalent concentration and the 2.5g sodium sulfate equivalent concentration were broken down and compared with a box containing pure sulfuric acid. Once the plates were removed from the battery boxes there rinsed under DI water for approximately 4 hours to remove any acid from the plates. After rinsing the plates were placed in a vacuum oven at 60°C overnight to remove any water and prevent further reactions from taking place.

For the SEM/EDS images sections of the negative plate were removed corresponding to positions 2 and 3 in Figure 18. The electron microscope used for the SEM and EDS images is a a Hitachi S-4800 with a 3 kV accelerating voltage. For the Energy Dispersive X-Ray Spectroscopy (EDS) uses x-rays to excite the surface of a sample and upon relaxation emission spectra are gathered by the sensor. Since each element has a unique atomic structure, the emission from each element is also unique. This method can be used to effectively analyze the elemental makeup of the surface of a sample.

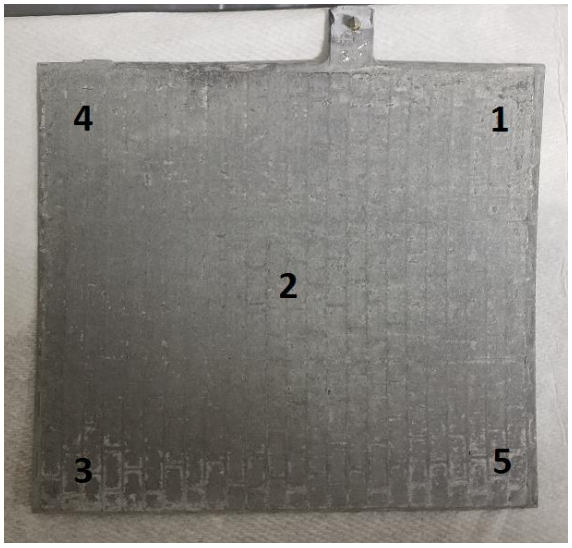

Figure 18: Negative Plate Sample Locations

3 Results and Discussion

3.1 Charge Acceptance

In the first round of testing all the battery boxes were filled with sulfuric acid with a metal ion concentration of 0.2112 M, or, in the case of copper, bismuth, and tin, saturated. Figure 19 shows the results of the four charge acceptance steps from the five-cycle test for each of the additives tested.

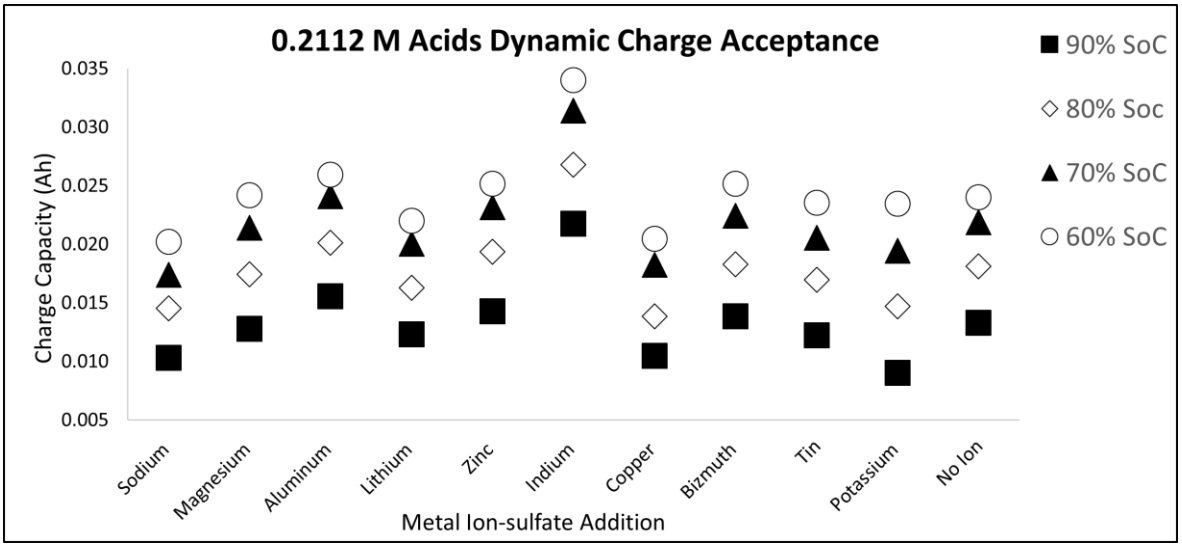

Figure 19: High Concentration Dynamic Charge Acceptance plot, All Acids

The plot in Figure 18 illustrates the typical behavior of charge acceptance. A table of the values in Figure 18 can be found in the Appendix. As the battery is further discharged it is increasingly capable of accepting a larger charge. This behavior is the main reason why new applications of lead-acid batteries need to operate at a partial state of charge: to be able to take advantage of the charging energy availably during micro-hybrid driving. The second thing the plot displays is the large difference in the effect these metal ions can have on the charge acceptance behavior of the lead acid cells. Another notable point displayed in Figure 20 is the charge acceptance capability of the sodium sulfate electrolyte. In comparison with the other electrolyte additives used, sodium sulfate has the poorest charge acceptance behavior. Considering sodium sulfate's use as an additive for the past few decades has been to reduce shorting and improve cold cranking performance, it is not surprising that it does not have exceptional charge acceptance effects.

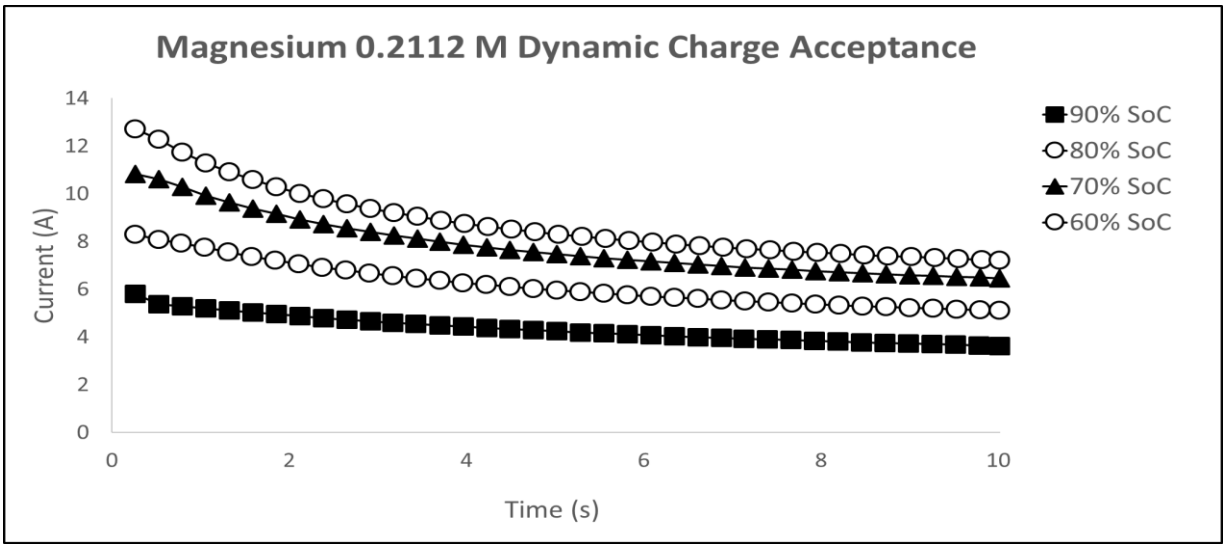

Figure 20:Charge acceptance plot for magnesium across four different DoDs

Figure 19 shows an expanded view of the four charge acceptance steps for the zinc sulfate additive electrolyte. This plot is representative of the charge acceptance steps seen by all the acids used in this experiment. With the voltage held at 2.4V the current spikes to a high

initial value and decays down to what would eventually be a constant current that would continue to decay as the battery SoC increases. The charge capacity is calculated by the Arbin software by integrating the Time vs Current curve to give a value in Ah that can easily be compared with other tests.

Based on the high charge capacities seen by the aluminum sulfate and zinc sulfate boxes and the low likelihood of indium sulfate's industrial application due to its high cost, further testing at lower concentrations of aluminum sulfate and zinc sulfate were performed. Figures 21 and 22 show the charge acceptance steps for these two additives at a range of concentrations.

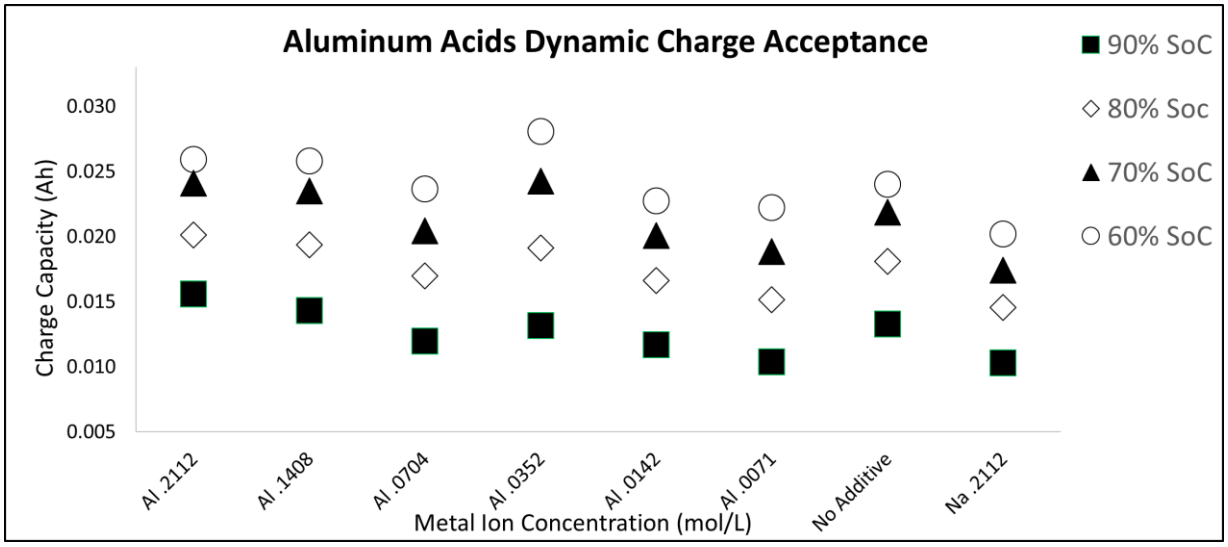

Figure 21: Aluminum Sulfate Charge Acceptance for several concentrations

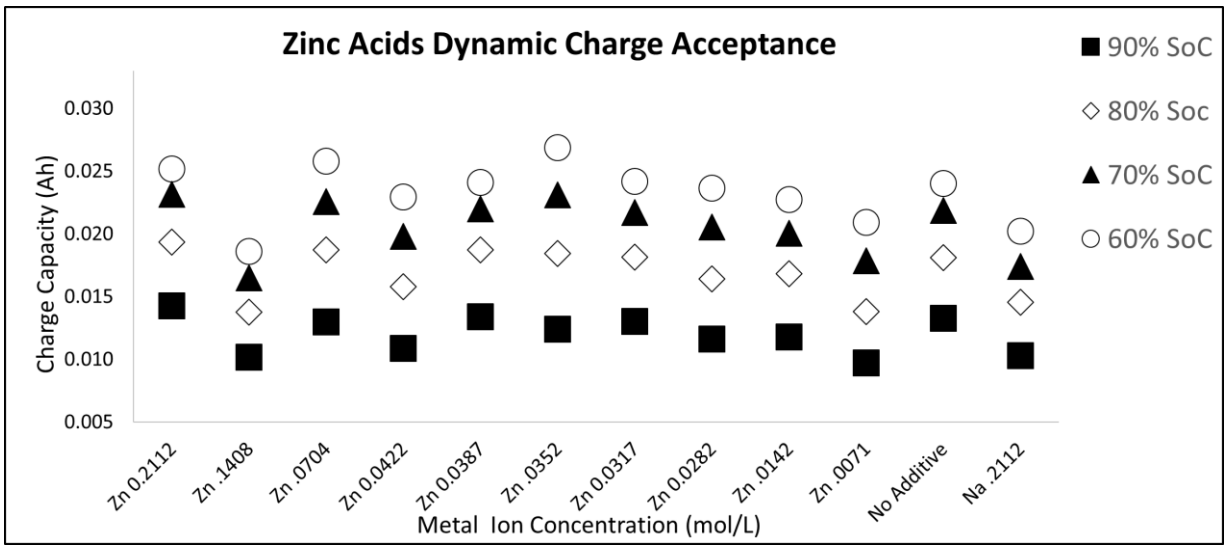

Figure 22: Zinc Sulfate Charge Acceptance for Several Concentrations

Tables containing the values for Figures 21 and 22 can be found in the Appendix.

Running the five-cycle test revealed that the effect of the concentration on the charge acceptance did not have a linear relationship. For both the aluminum sulfate and the zinc sulfate the 0.0352 $\frac{mol}{L}$ concentration gave the highest charge acceptance at the 60% SoC level. After this new trend emerged the entire set of acids were also tested at the 0.0352 $\frac{mol}{L}$ and the results of that test can be seen below in Figure 23.

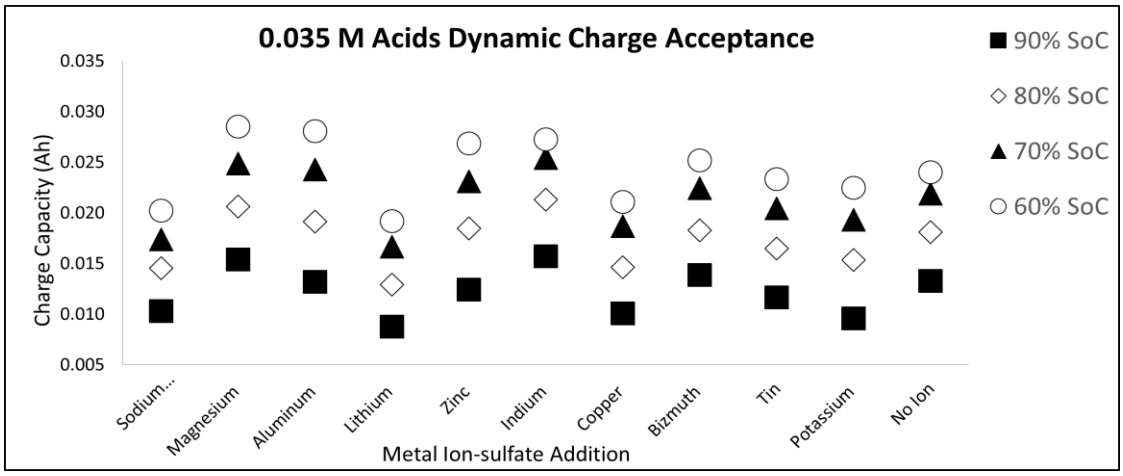

Figure 23: Charge acceptance of Metal-Ion Sulfates at the 0.035 M level

Figure 22 shows that three ions showed heightened charge acceptance behavior at the 0.0352 $\frac{mol}{L}$ level: Aluminum, Zinc, and Magnesium. Indium, which showed by far the highest charge acceptance at the 0.2112 $\frac{mol}{L}$ level, shows a lower charge acceptance than magnesium and aluminum at this lower level. This trend implies that for each element there is likely a different ideal concentration for each ion that will show the highest charge acceptance value. A table with the values from Figure 23 is available in the Appendix. Figure 24 shows the charge acceptance steps of magnesium at this lower concentration.

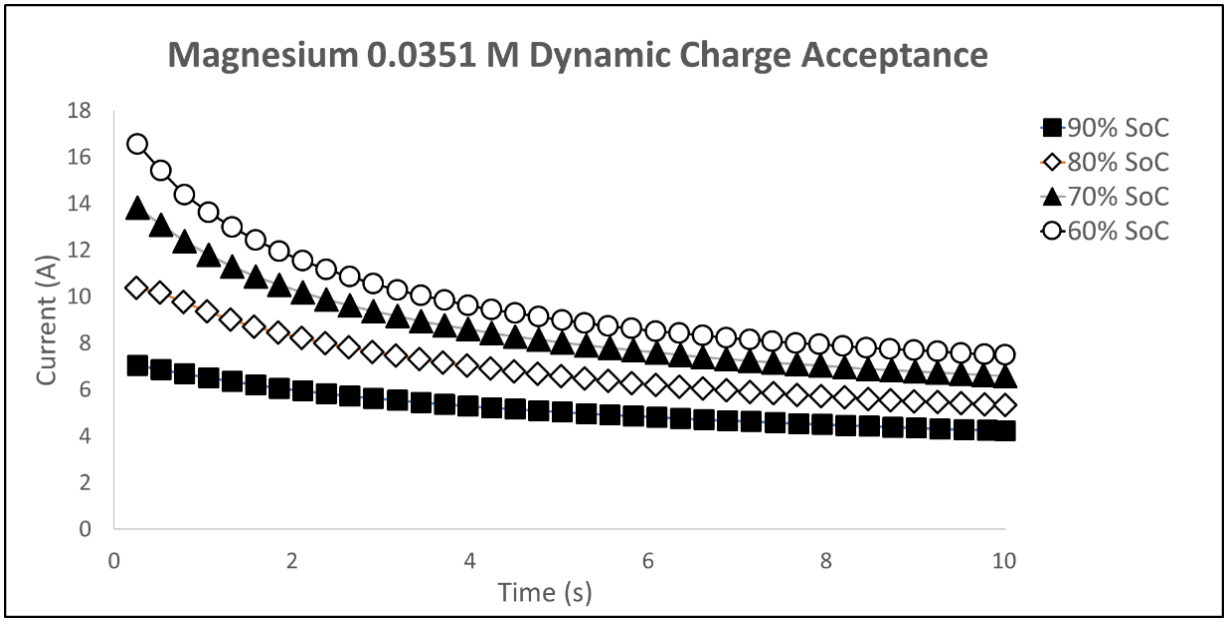

Figure 24: Charge acceptance plot for 0.0351 M magnesium across four different DoDs.

When comparing Figure 24 to Figure 20, two important differences arise. The first is that the initial current at the lower concentration is much higher. The second is that the current level approached during the current decay is higher at all levels of discharge.

3.2 Cold Cranking

The cold cranking test was run on many of the acids at their 0.0352 $\frac{mol}{L}$ or at a saturated concentration if their solubility was very low. Figure 25 show a plot of the cold cranking discharge capacity of these acids.

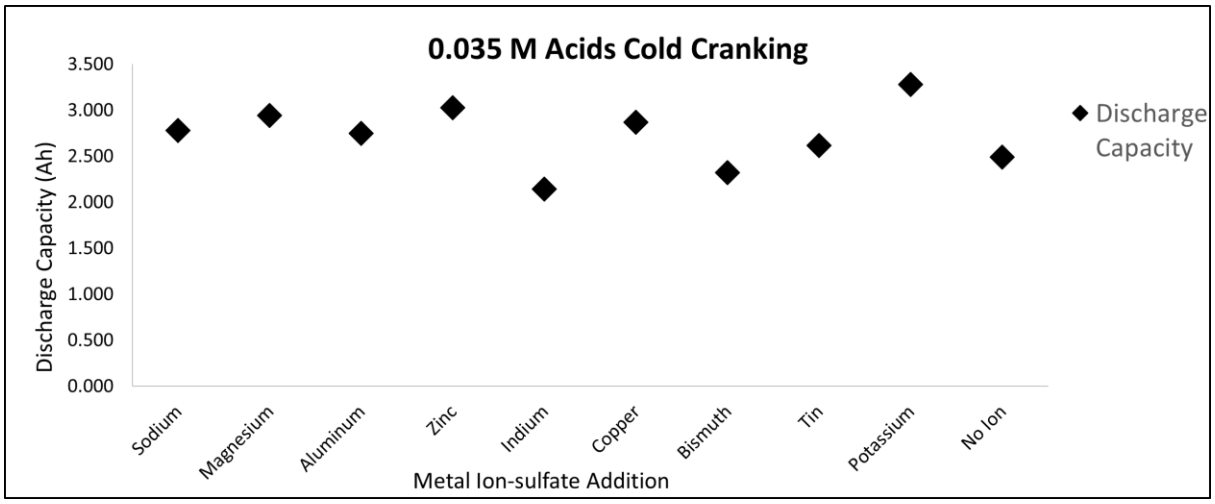

Figure 25: Cold cranking capacity of low concentration acids.

The sodium data point on the left end of the plot is for the reference acid. The magnesium and zinc both have slightly improved discharge capacities over the reference acid and aluminum has a slight decrease. Based on the small differences in the charge capacity of these three acids, the added charge capacity they provide does not come with a detrimental effect on the cells cold cranking abilities compared to the reference cell.

3.3 ICP-OES Analysis

For the ICP-OES analysis calibration curves for aluminum and zinc were calculated from 4 standard solutions. A blank HNO_3 standard and standard solutions of 2, 5 and 10 ppm of aluminum and standard solutions containing 2, 10, and 20 ppm of zinc. The electrolyte solutions were diluted by a factor of 300 and the dissolved plate samples were diluted by a factor of 300 to evaluate the lead content and by a factor of 50 to evaluate the ion content. Tables 7 and 8 shows the results of the electrolyte analysis.

Al Concentration	**Pure Acid ($\frac{mg}{L}$)**	**Post Formation acid($\frac{mg}{L}$)**
0.2112 $\frac{mol}{L}$	17.00	19.79
0.0352 $\frac{mol}{L}$	1.88	1.99
No Additive	0.00	0.163

Table 7: ICP-OES results for aluminum content of electrolyte at 300 times dilution.

Zn Concentration	**Pure Acid ($\frac{mg}{L}$)**	**Post Formation acid($\frac{mg}{L}$)**
0.2112 $\frac{mol}{L}$	45.03	40.65
0.0352 $\frac{mol}{L}$	7.47	6.22
No Additive	-0.10	0.03

Table 8:ICP-OES results for zinc content of electrolyte at 300 times dilution.

For the ICP analysis of the lead plates 0.5g of the powdered lead plate was dissolved in nitric acid for the aluminum plates and 0.2g of the powdered lead was dissolved in nitric acid for the zinc plates and the no additive plates. The solution was diluted by a factor of 300 to analyze the lead concentration and by a factor of 50 to analyze the aluminum and zinc concentration in the plates.

Concentration	**Aluminum** ($\frac{mg}{L}$)	**Zinc**($\frac{mg}{L}$)	**Lead**($\frac{mg}{L}$)
Aluminum 0.2112 $\frac{mol}{L}$	0.01	0.02	26.52
Aluminum 0.0352 $\frac{mol}{L}$	-0.01	0.05	27.00
No Additive	0.04	0.00	12.60
Zinc 0.2112 $\frac{mol}{L}$	0.00	0.13	10.81
Zinc 0.0352 $\frac{mol}{L}$	-0.02	-0.03	10.65

Table 9: ICP-OES results for zinc, aluminum, and lead concentration in lead plates

The results in Tables 7 and 8 show some interesting behavior with the concentration of the target additives in the electrolyte. The expectation would be that if the additives form some sort of alloy with the lead plates or plate the surface of either plate there would be a drop in their concentration after formation. If the ion additives act as a catalyst then the expectation would be for the concentration to remain the same after the formation process. Looking at the aluminum concentrations in Table 7, the concentration of aluminum in those samples increased slightly for both the 0.2112 $\frac{mol}{L}$ sample and the .0352 $\frac{mol}{L}$ sample. An increase in the concentration after formation is expected since water is lost during the formation process.

The zinc concentrations are more interesting. For both the 0.2112 $\frac{mol}{L}$ sample and the 0.0352 $\frac{mol}{L}$ sample the concentration of zinc in the electrolyte decreased by over 10%. Since the zinc concentration has decreased, the zinc may have been left of the surface of the plate in one form or another. The results in Table 9 show the concentration of ions found in the lead plates themselves. At the dilution factor of 300, lead showed up with the expected concentration in each sample but the concentration of the aluminum and zinc ions was too low for the sensitivity

of the sensor. For this ICP-OES machine the sensor is no longer accurate at levels below 0.5 ppm. To get the samples in the appropriate range the plate samples were diluted by a factor of 50. At this dilution, there was still no aluminum or zinc detected in the lead plate samples.

3.4 SEM and EDS Analysis

To further understand the interactions between the electrolyte additives and the negative plate in a lead-acid battery, SEM images and EDS mapping were used. The images in Figure 26 show the structure on the plate surface from each ion at the 0.0352M concentration at two magnification levels.

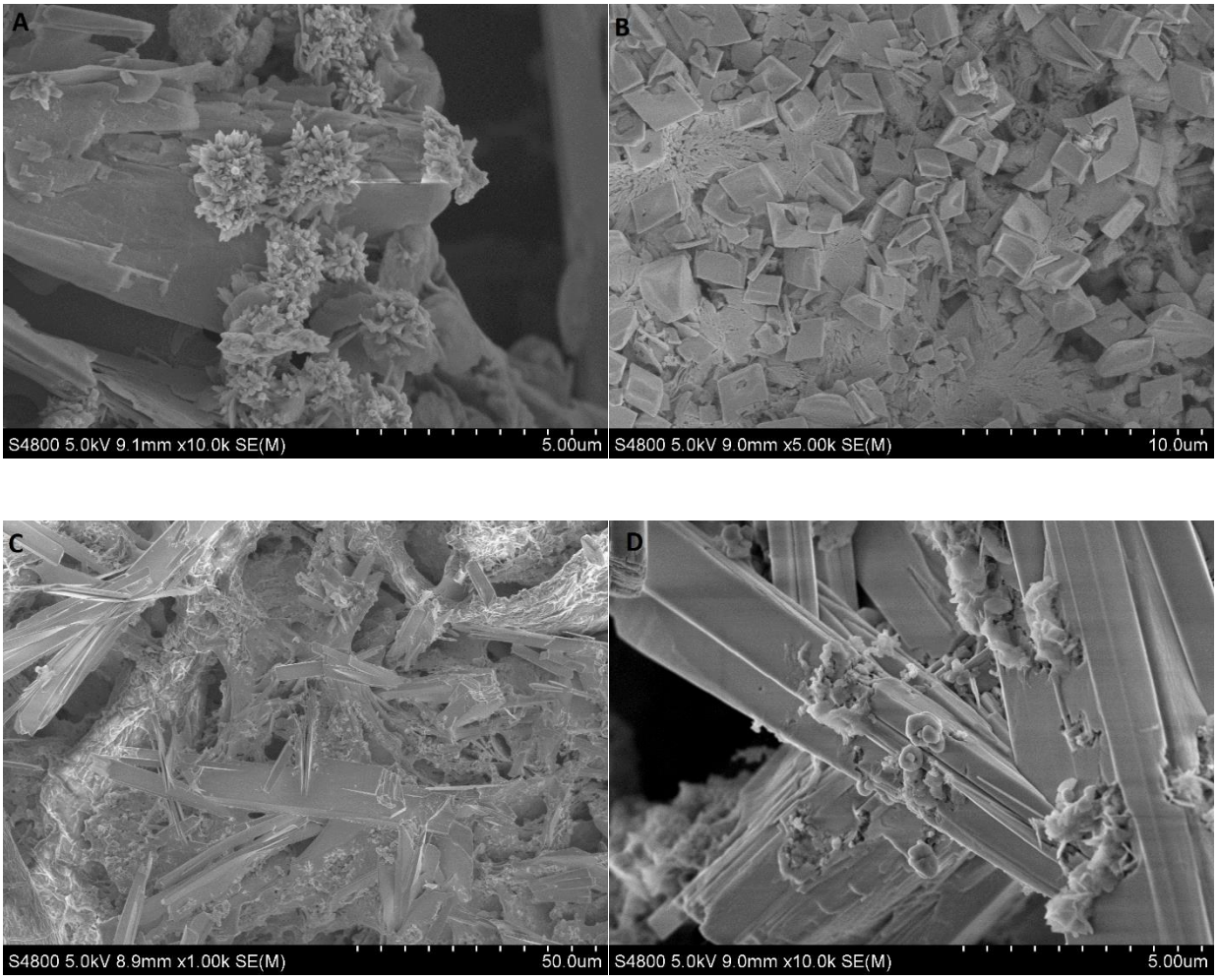

Figure 26: SEM images of negative lead plate. (A) Zinc low concentration, location 2, (B) Zinc low concentration, location 3, (C) Aluminum low concentration, location 2, and (D) Aluminum low concentration, position 3.

The images show the presence of very small lead sulfate crystals. Since the images are taken after the cells had been fully recharged and only put through 4 charge/discharge cycles and 4 separate SoC charge pulses before being fully charge, the presence of a small amount of lead sulfate is expected. To show the presence of the target elements the samples were mapped using EDS. In Figure 26 (A) the small spiked clusters are lead sulfate. The other crystalline structures seen in the SEM images are the various lead compounds typically found in the negative active mass. The images do not show distinct differences between the different types of electrolyte that

were used, only that there is very little presence of lead sulfate on the plate surface and the lead sulfate that does exist is found in very small crystals.

The spectra below in Figure 27 shows the EDS results for the plate sample with no additive in the electrolyte. Data collected from EDS analysis is plotted with the energy in electron volts on the X-axis and the count of x-rays that hit the sensor per second on the Y-axis. The spectrum shows no peaks for the zinc or aluminum and very large peaks for lead.

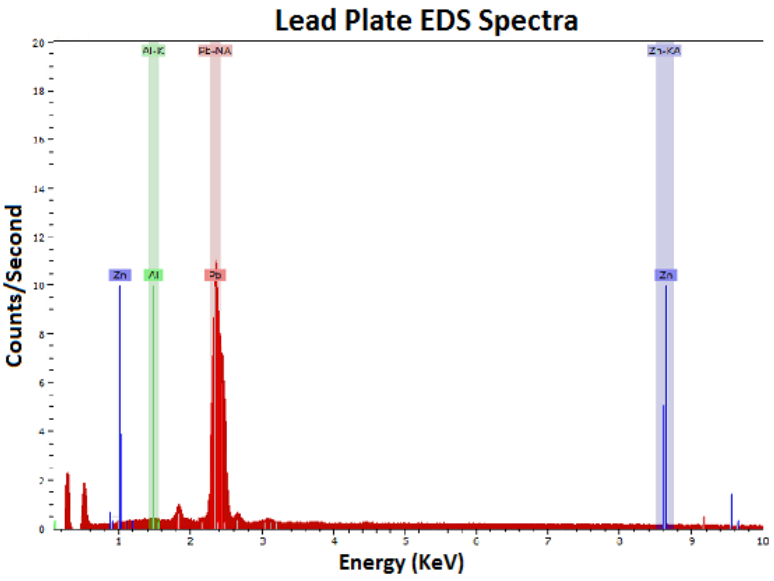

Figure 27: EDS spectra for the no additive negative plate.

The spectra for the other plates resemble Figure 27 with no meaningful peaks representing the presence of zinc or aluminum on the plate surface. The mapping feature also failed to show concentrations of zinc or aluminum on the plate surface. From the SEM and EDS analysis, zinc and aluminum do not appear to be present on the surface of the negative plate at a fully charged state.

4 Conclusion

The previous experiment has shown that the presence of metal ions in the electrolyte can have large effects on the behavior of an AGM lead-acid battery. Using 1.24 g/mL density sulfuric acid with 15g/L (0.2112mol/L of sodium) of sodium sulfate added as an industry benchmark, several new electrolytes were made using different metal-sulfate salts. The concentration of the metal ions in the solution played a large part in the determining the charge acceptance behavior of the battery. The DoD of the battery also effects the change in charge acceptance behavior. Using aluminum at the 0.0352 mol/L level, the charge acceptance value at the 60% SoC was the largest of any aluminum concentration. At the 90%SoC, the highest charge acceptance value was found using the 0.2112 mol/Lof aluminum ions. This pattern also occurred with the zinc sulfate acids with the 0.2112 mol/L zinc acid showing the best charge acceptance behavior at 90% SoC and the 0.0352mol/L zinc acid showing the best charge acceptance behavior at 60% SoC.

Except for indium, all additives showed lower charge acceptance value at the 0.2112mol/L concentration than at lower levels. The increase in charge acceptance with the decreasing concentration is not linear and shows the highest charge acceptance values for most of the additives at the 0.0352mol/L concentration.

A general trend also appeared based on the oxidation state of the metal ions. Except for copper, the ions with an oxidation state of +1 (potassium, lithium, and sodium) showed the worst performance for charge acceptance at low concentrations. Copper, with an oxidation state of +2, had a very high shorting rate and exhibited low charge acceptance values. The best performing ions have either a +2 or +3 oxidation state. A trend did not appear based on the weights of the

ion with weights of the best ions ranging from 12 g/mol for magnesium to 49 g/mol for indium and the worst ions ranging from 3g/mol for lithium and 83 g/mol for bismuth.

The electrical testing performed has shown that different metal ions can cause significant effects on the performance of a lead-acid battery and that trends exist between oxidation state, concentration, and charge acceptance behavior. The mechanism behind how these ions affect charge acceptance is not elucidated through electrical testing.

The main goal of the electrical testing was to show that ions can affect charge acceptance behavior. The SEM-EDS and ICP-OES analysis was intended to shed some light on the mechanism by which these changes occur. The results from these two techniques showed that there was little lead sulfate accumulation on the plates, which was expected, and that the metal ions were not present on the plate surface at a full state of charge. From these two analytical techniques there is not enough information to make any firm conclusions about the mechanism behind metal ions improving charge acceptance.

In all, the addition of specific metal ions to the electrolyte can improve the batteries charge acceptance capability, which is key parameter for improving lead-acid batteries for micro-hybrid use. The tests performed here have shown have shown substantial increases in charge acceptance behaviors over conventional lead-acid battery electrolyte. The best performing ions (zinc, magnesium, and aluminum) have showed charge acceptance increases of 32-41% at a 60% SoC and increases of 24-51% at the 90% SoC.

4.1 Future Work

The previous tests show that single metal ions can strongly affect the charge acceptance behavior in lead acid batteries. What the testing does not show are the long-term

effects these ions may have, the impact of using several ions together, and the mechanism behind the changes in charge acceptance behavior. Based on this, there are three clear paths forward to better understand the impact metal ions can have.

The first path involves long term testing to evaluate the applicability of these additives in an industrial setting. If an ion additive provides great charge acceptance at the expense of cycle life or cold cranking performance, the benefits would not offset the losses. To better understand the long-term effects, full scale batteries should be run through a variety of tests that would evaluate cycle life under normal and micro-hybrid cycling, water consumption, and cold cranking.

A second area of further study would be to evaluate the mechanism for the changes in charge acceptance behavior with the addition of metal sulfates. Moving forward with this testing, several assumptions based on the results from the previous experiments will be made. The first is that the metal sulfates are not causing a change in charge acceptance through changes in gas generation. This assumption is based on the weight loss during the formation process remaining constant regardless of the additives used. The second assumption is that the metal ions are not changing the charge acceptance behavior by changing the conductivity of the plates. The ICP and SEM-EDS data gathered from negative plates formed with both zinc and aluminum additives showed no presence of either ion within or on the surface of the plate. The assumed mechanism for changing the charge acceptance with metal sulfate additives is changing the size, geometry, or distribution of the lead sulfate crystals grown during discharge, much like was seen

in the evaluation of negative plates after use with various surfactant additives [54].

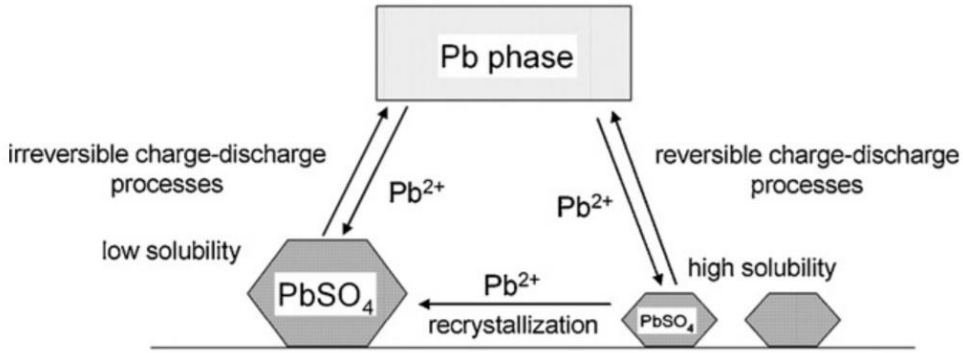

Figure 28:Lead sulfate crystal formation.[60]

As Figure 28 shows the pathways to lead sulfate crystal growth. Small crystals are easily dissolved during the typical charge process while large crystals are more difficult to dissolve with typical charging processes. With this in mind, specific charging and discharging profiles will be used to encourage the growth of larger lead sulfate crystals. To grow large crystals, a combination of low current discharges and low current recharges encourage larger crystal growth. Running batteries through these cycles in 10-14 day increments may show the progression of crystal growth and, if successful, meaningful differences may be seen between the size, shape, and dispersion of the crystals between the different metal sulfate additives.

Works Cited

[1] "Transportation Statistics Annual Report 2017," U.S. Department of Transportation, Bureau of Transportation Statistics, Washington, DC, 2017.

[2] D. S. Ginley and D. Cahen, Eds., *Fundamentals of Materials for Energy and Environmental Sustainability*. Cambridge University Press.

[3] D. Pavlov, *Lead-acid batteries: science and technology: a handbook of lead-acid battery technology and its influence on the product*. Amsterdam ; Singapore: Elsevier Science Ltd, 2011.

[4] B. Culpin, "The Lead Acid Battery - 130 Years Old and Still Improving," *Chem. Ind.*, pp. 826–829, 1989.

[5] "Overview of the ALABC 2016-2018 Program Proposal." Advanced Lead Acid Battery Consortium, 2015.

[6] E. P. Finger and D. D. P. Boden, "Battery Book 2," *EV Battery Monitoring*. [Online]. Available: http://evbatterymonitoring.com/BatteryBook2/Battery_Book_2.htm. [Accessed: 05-Mar-2018].

[7] J. Devitt, "An account of the development of the first valve-regulated lead/acid cell," *J. Power Sources*, vol. 64, no. 1–2, pp. 153–156, Feb. 1997.

[8] J. Garche, K. Eckhard, P. Moseley. T., and D. Rand A. J., Eds., *Lead-Acid Batteries for Future Automobiles*. 50 Hampshire Street, 5th Floor, Cambridge, MA 02139, United States: Elsevier, 2017.

[9] G. C. Zguris, "A broad look at separator material technology for valve-regulated lead/acid batteries," *J. Power Sources*, vol. 73, no. 1, pp. 60–64, 1998.

[10] P. Weissler, "AGM battery takes primary role for idle stop-start in microhybrids - SAE International," *SAE International*, 14-Feb-2012. [Online]. Available: http://articles.sae.org/10667/. [Accessed: 12-Apr-2018].

[11] "U.S. Energy Facts - Energy Explained, Your Guide To Understanding Energy - Energy Information Administration." [Online]. Available: https://www.eia.gov/energyexplained/?page=us_energy_home#tab3. [Accessed: 12-Apr-2018].

[12] E. Karden, P. Shinn, P. Bostock, J. Cunningham, E. Schoultz, and D. Kok, "Requirements for future automotive batteries – a snapshot," *J. Power Sources*, vol. 144, no. 2, pp. 505–512, Jun. 2005.

[13] J. Albers, E. Meissner, and S. Shirazi, "Lead-acid batteries in micro-hybrid vehicles," *J. Power Sources*, vol. 196, no. 8, pp. 3993–4002, Apr. 2011.

[14] G. Zhu *et al.*, “Materials insights into low-temperature performances of lithium-ion batteries,” *J. Power Sources*, vol. 300, pp. 29–40, Dec. 2015.

[15] B. Swain, “Recovery and recycling of lithium: A review,” *Sep. Purif. Technol.*, vol. 172, pp. 388–403, Jan. 2017.

[16] X. Guo, X. Cao, G. Huang, Q. Tian, and H. Sun, “Recovery of lithium from the effluent obtained in the process of spent lithium-ion batteries recycling,” *J. Environ. Manage.*, vol. 198, pp. 84–89, Aug. 2017.

[17] H. Vikström, S. Davidsson, and M. Höök, “Lithium availability and future production outlooks,” *Appl. Energy*, vol. 110, pp. 252–266, Oct. 2013.

[18] T. P. Narins, “The battery business: Lithium availability and the growth of the global electric car industry,” *Extr. Ind. Soc.*, vol. 4, no. 2, pp. 321–328, Apr. 2017.

[19] C. Helbig, A. M. Bradshaw, L. Wietschel, A. Thorenz, and A. Tuma, “Supply risks associated with lithium-ion battery materials,” *J. Clean. Prod.*, vol. 172, pp. 274–286, Jan. 2018.

[20] K. Fehrenbacher, “Why Tesla’s grid batteries will use two different chemistries,” *Fortune*, 18-May-2015. [Online]. Available: http://fortune.com/2015/05/18/tesla-grid-batteries-chemistry/. [Accessed: 12-Apr-2018].

[21] J. Farchy and M. Gurman, “Apple in Talks to Buy Cobalt Directly From Miners,” *Bloomberg.com*, 21-Feb-2018.

[22] E. Airhart, “Alternatives to Cobalt, the Blood Diamond of Batteries,” *Wired*, 07-Jun-2018.

[23] “Electric Cars, Solar Panels & Clean Energy Storage | Tesla.” [Online]. Available: https://www.tesla.com/. [Accessed: 12-Apr-2018].

[24] A. B. C. News, “NTSB investigating Tesla crash, fire that killed 2 teens,” *ABC News*, 10-May-2018. [Online]. Available: https://abcnews.go.com/US/ntsb-investigating-tesla-crash-fire-killed-florida-teens/story?id=55062449. [Accessed: 24-Jul-2018].

[25] A. B. C. News, “Why Did the Tesla Car Catch on Fire?,” *ABC News*, 03-Oct-2013. [Online]. Available: https://abcnews.go.com/Technology/tesla-model-catch-fire/story?id=20462128. [Accessed: 24-Jul-2018].

[26] F. Lambert, “Tesla will update the Model S software for safer charging following a Supercharger fire,” *Electrek*, 17-Mar-2016. .

[27] F. Lambert, “Tesla Model S catches on fire during a test drive in France,” *Electrek*, 15-Aug-2016. .

[28] A. Kieler, “Feds Announce Airplane Ban for all Samsung Galaxy Note7 Phones,” *Consumer Reports*. [Online]. Available: http://consumerist.com/2016/10/14/feds-to-announce-airplane-ban-for-all-samsung-galaxy-note-7-phones/. [Accessed: 12-Apr-2018].

[29] U. Irfan, “How Lithium Ion Batteries Grounded the Dreamliner,” *Scientific American*. [Online]. Available: https://www.scientificamerican.com/article/how-lithium-ion-batteries-grounded-the-dreamliner/. [Accessed: 12-Apr-2018].

[30] “Nissan Cars, Trucks, Crossovers, & SUVs | Nissan USA.” [Online]. Available: https://www.nissanusa.com/?dcp=psn.5870000285684922&gclid=EAIaIQobChMI4K-fn5vH2gIVBrXACh2-hASnEAAYASAAEgIopPD_BwE&gclsrc=aw.ds&dclid=CKLP0qGbx9oCFUG-TwodXK8PUA. [Accessed: 19-Apr-2018].

[31] U. of Sheffield, “Dynamic Charge Acceptance Testing - Research - Centre for Research into Electrical Energy Storage & Applications - The University of Sheffield.” [Online]. Available: https://www.sheffield.ac.uk/creesa/research/dynamic-charge. [Accessed: 12-Apr-2018].

[32] A. Jaiswal and S. C. Chalasani, “The role of carbon in the negative plate of the lead–acid battery,” *J. Energy Storage*, vol. 1, pp. 15–21, Jun. 2015.

[33] P. T. Moseley, “Consequences of including carbon in the negative plates of Valve-regulated Lead–Acid batteries exposed to high-rate partial-state-of-charge operation,” *J. Power Sources*, vol. 191, no. 1, pp. 134–138, Jun. 2009.

[34] D. Pavlov and P. Nikolov, “Capacitive carbon and electrochemical lead electrode systems at the negative plates of lead–acid batteries and elementary processes on cycling,” *J. Power Sources*, vol. 242, pp. 380–399, Nov. 2013.

[35] E. Ebner *et al.*, “Carbon blacks for lead-acid batteries in micro-hybrid applications – Studied by transmission electron microscopy and Raman spectroscopy,” *J. Power Sources*, vol. 222, pp. 554–560, Jan. 2013.

[36] J. Xiang, P. Ding, H. Zhang, X. Wu, J. Chen, and Y. Yang, “Beneficial effects of activated carbon additives on the performance of negative lead-acid battery electrode for high-rate partial-state-of-charge operation,” *J. Power Sources*, vol. 241, pp. 150–158, Nov. 2013.

[37] R. Marom, B. Ziv, A. Banerjee, B. Cahana, S. Luski, and D. Aurbach, “Enhanced performance of starter lighting ignition type lead-acid batteries with carbon nanotubes as an additive to the active mass,” *J. Power Sources*, vol. 296, pp. 78–85, Nov. 2015.

[38] S. W. Swogger, P. Everill, D. P. Dubey, and N. Sugumaran, “Discrete carbon nanotubes increase lead acid battery charge acceptance and performance,” *J. Power Sources*, vol. 261, pp. 55–63, Sep. 2014.

[39] K. K. Chawla, *Composite Materials*, Third Edition. Springer, 2013.

[40] J. Valenciano, A. Sánchez, F. Trinidad, and A. F. Hollenkamp, “Graphite and fiberglass additives for improving high-rate partial-state-of-charge cycle life of valve-regulated lead-acid batteries,” *J. Power Sources*, vol. 158, no. 2, pp. 851–863, Aug. 2006.

[41] D. Pavlov, T. Rogachev, P. Nikolov, and G. Petkova, “Mechanism of action of electrochemically active carbons on the processes that take place at the negative plates of lead-acid batteries,” *J. Power Sources*, vol. 191, no. 1, pp. 58–75, Jun. 2009.

[42] V. E, “Effects of phosphoric acid additions on the behavior of the lead-acid cell,” *J. Power Sources*, vol. 24, pp. 171–184, 1988.

[43] K. Saminathan, N. Jayaprakash, B. Rajeswari, and T. Vasudevan, “Influence of phosphoric acid on the grid alloys of positive plates in the lead acid battery system: A comparative study,” *J. Power Sources*, vol. 160, no. 2, pp. 1410–1413, Oct. 2006.

[44] J. Garche, H. Döring, and K. Wiesener, “Influence of phosphoric acid on both the electrochemistry and the operating behaviour of the lead/acid system,” *J. Power Sources*, vol. 33, no. 1–4, pp. 213–220, 1991.

[45] M. S. Yazd, A. Molazemi, and M. H. Moayed, “The effects of different additives in electrolyte of AGM batteries on self-discharge,” *J. Power Sources*, vol. 158, no. 1, pp. 705–709, Jul. 2006.

[46] G. W. Mao and A. Sabation, “LEAD-ACID STORAGE BATTERY CAPABLE OF ACTIVATION BY THE ADDITION OF ELECTROLYTE,” 3948680.

[47] J. Yu, Z. Qian, M. Zhao, Y. Wang, and L. Niu, “Effects of sodium sulfate as electrolyte additive on electrochemical performance of lead electrode,” *Chem. Res. Chin. Univ.*, vol. 29, no. 2, pp. 374–378, Apr. 2013.

[48] L. Rekha, M. Venkateswarlu, K. S. N. Murthy, and M. Jagadish, “Sodium Sulphate as an Electrolyte Additive and its Influence on the Performance of the Lead Acid Battery,” *Int. J. Sci. Res.*, vol. 6, no. 8, pp. 517–520, 2017.

[49] JIS D 5301:2006 (E), “Lead-acid Starter Batteries.” Japanesa Standards Association.

[50] D. A. J. Rand, Ed., *Valve-regulated lead-acid batteries*, 1st ed. Amsterdam ; Boston: Elsevier, 2004.

[51] Y. Zeng, J. Hu, W. Ye, W. Zhao, G. Zhou, and Y. Guo, “Investigation of lead dendrite growth in the formation of valve-regulated lead-acid batteries for electric bicycle applications,” *J. Power Sources*, vol. 286, pp. 182–192, Jul. 2015.

[52] N. Vangapally, S. A. Gaffoor, and S. K. Martha, “Na 2 EDTA chelating agent as an electrolyte additive for high performance lead-acid batteries,” *Electrochimica Acta*, vol. 258, pp. 1493–1501, Dec. 2017.

[53] “Surfactant | chemical compound,” *Encyclopedia Britannica*. [Online]. Available: https://www.britannica.com/science/surfactant. [Accessed: 21-Mar-2018].

[54] R. K. Ghavami, F. Kameli, A. Shirojan, and A. Azizi, “Effects of surfactants on sulfation of negative active material in lead acid battery under PSOC condition,” *J. Energy Storage*, vol. 7, pp. 121–130, Aug. 2016.

[55] H. Brown and H. Woods, “Method for Improving Electric Storage Batteries,” 2857295, 21-Oct-1958.

[56] Z. Shi, Y.-H. Zhou, and C.-S. Cha, “Influence of perfluorinated surfactants on the positive active-material of lead/acid batteries,” *J. Power Sources*, vol. 70, no. 2, pp. 205–213, Feb. 1998.

[57] N. Boudieb, M. Bounoughaz, and A. Bouklachi, “The Effect of Surfactants on the Efficiency of Lead Acid Batteries,” *Procedia - Soc. Behav. Sci.*, vol. 195, pp. 1618–1622, Jul. 2015.

[58] J. Claus, F. O. Sommer, and U. Kragl, “Ionic liquids in biotechnology and beyond,” *Solid State Ion.*, vol. 314, pp. 119–128, Jan. 2018.

[59] B. Rezaei, S. Mallakpour, and M. Taki, “Application of ionic liquids as an electrolyte additive on the electrochemical behavior of lead acid battery,” *J. Power Sources*, vol. 187, no. 2, pp. 605–612, Feb. 2009.

[60] D. Pavlov and P. Nikolov, “Lead-Carbon Electrode with Inhibitor of Sulfation for Lead-Acid Batteries Operating in the HRPSoC Duty,” *J. Electrochem. Soc.*, vol. 159, no. 8, pp. A1215–A1225, Jan. 2012.

Appendix: Charge Acceptance and Cold Cranking Raw Data

	90% SoC		80% SoC		70% SoC		60% SoC	
Additive	**Current (A)**	**Cap. (Ah)**	**Current (A)**	**Cap. (Ah)**	**Current (A)**	**Cap. (Ah)**	**Current (A)**	**Cap. (Ah)**
Sodium	3.38	0.0103	4.63	0.0145	5.45	0.0174	6.28	0.0202
Magnesium	3.77	0.0128	5.06	0.0174	6.15	0.0214	6.98	0.0242
Aluminum	4.72	0.0156	5.78	0.0201	7.00	0.0241	7.61	0.0259
Lithium	3.89	0.0123	5.12	0.0163	6.23	0.0200	6.86	0.0220
Zinc	4.14	0.0143	5.61	0.0194	6.80	0.0232	7.45	0.0252
Indium	6.70	0.0217	8.26	0.0268	9.77	0.0314	10.73	0.0340
Copper	3.70	0.0105	4.82	0.0138	6.32	0.0182	7.12	0.0205
Bismuth	3.98	0.0138	5.31	0.0183	6.57	0.0224	7.37	0.0252
Tin	3.92	0.0122	5.34	0.0170	6.42	0.0206	7.33	0.0236
Potassium	3.41	0.0090	5.39	0.0147	6.78	0.0194	7.72	0.0235
No Ion	3.88	0.0133	5.33	0.0181	6.46	0.0219	7.10	0.0240

Table 10: Raw Data for 0.2112 M Charge Acceptance Plot

	90% SoC		80% SoC		70% SoC		60% SoC	
Additive	**Current (A)**	**Cap. (Ah)**	**Current (A)**	**Cap. (Ah)**	**Current (A)**	**Cap. (Ah)**	**Current (A)**	**Cap. (Ah)**
Al .2112	4.72	0.0156	5.78	0.0201	7.00	0.0241	7.61	0.0259
Al .1408	4.33	0.0143	5.63	0.0194	6.93	0.0235	7.71	0.0258
Al .0704	3.76	0.0120	5.08	0.0170	6.08	0.0204	7.07	0.0236
Al .0352	3.98	0.0132	5.63	0.0191	7.08	0.0243	8.23	0.0281
Al .0142	3.64	0.0117	4.96	0.0166	5.90	0.0201	6.76	0.0228
Al .0071	3.23	0.0104	4.61	0.0151	5.66	0.0189	6.77	0.0222
None	3.88	0.0133	5.33	0.0181	6.46	0.0219	7.10	0.0240
Na .2112	3.38	0.0103	4.63	0.0145	5.45	0.0174	6.28	0.0202

Table 11: Raw Data for Aluminum Acids Charge Acceptance Plot

	90% SoC		80% SoC		70% SoC		60% SoC	
Additive	**Current (A)**	**Cap. (Ah)**	**Current (A)**	**Cap. (Ah)**	**Current (A)**	**Cap. (Ah)**	**Current (A)**	**Cap. (Ah)**
Zn 0.2112	4.14	0.0143	5.61	0.0194	6.80	0.0232	7.45	0.0252
Zn .1408	3.83	0.0102	5.15	0.0137	6.24	0.0165	7.11	0.0186
Zn .0704	3.82	0.0130	5.44	0.0187	6.59	0.0226	7.65	0.0258
Zn 0.0422	3.38	0.0109	4.82	0.0158	5.96	0.0198	6.91	0.0229
Zn 0.0387	4.09	0.0134	5.53	0.0187	6.44	0.0220	7.03	0.0241
Zn .0352	3.79	0.0124	5.36	0.0184	6.63	0.0231	7.77	0.0269
Zn 0.0317	3.93	0.0130	5.37	0.0181	6.44	0.0217	7.09	0.0242
Zn 0.0282	3.57	0.0116	4.94	0.0164	6.14	0.0205	7.08	0.0236
Zn .0142	3.55	0.0118	4.98	0.0168	5.90	0.0200	6.76	0.0227
Zn .0071	3.66	0.0097	5.17	0.0138	6.44	0.0178	7.56	0.0209
None	3.88	0.0133	5.33	0.0181	6.46	0.0219	7.10	0.0240

Table 12: Raw Values for Zinc Charge Acceptance Plot

	90% SoC		80% SoC		70% SoC		60% SoC	
Additive	**Current (A)**	**Cap. (Ah)**	**Current (A)**	**Cap. (Ah)**	**Current (A)**	**Cap. (Ah)**	**Current (A)**	**Cap. (Ah)**
Sodium (0.2212M)	3.38	0.0103	4.63	0.0145	5.45	0.0174	6.28	0.0202
Magnesium	4.49	0.0154	5.81	0.0206	6.96	0.0249	7.98	0.0285
Aluminum	3.98	0.0132	5.63	0.0191	7.08	0.0243	8.23	0.0281
Lithium	2.77	0.0088	3.98	0.0129	5.03	0.0167	5.74	0.0192
Zinc	3.79	0.0124	5.36	0.0184	6.63	0.0231	7.77	0.0269
Indium	4.69	0.0157	6.37	0.0213	7.74	0.0254	8.38	0.0273
Copper	3.18	0.0101	4.65	0.0146	5.93	0.0187	6.65	0.0211
Bismuth	3.98	0.0138	5.31	0.0183	6.57	0.0224	7.37	0.0252
Tin	3.55	0.0116	4.99	0.0165	6.14	0.0204	7.00	0.0234
Potassium	3.25	0.0096	4.76	0.0153	6.00	0.0193	6.88	0.0225
None	3.88	0.0133	5.33	0.0181	6.46	0.0219	7.10	0.0240

Table 13: Raw Values for 0.0352 Charge Acceptance Plot

Ion	**Time (S)**	**Cap. (Ah)**
Sodium	333.01	2.78
Magnesium	352.74	2.94
Aluminum	329.58	2.75
Zinc	362.90	3.02
Indium	257.26	2.14
Copper	343.94	2.87
Bismuth	278.25	2.32
Tin	314.01	2.62
Potassium	393.71	3.28
No Ion	298.75	2.49

Table 14: Cold Cranking Raw Values